Chapter IX

Insertion behavior of imidazolium and pyrrolidinium based ionic liquids into α and β-cyclodextrins: Mechanism and factors leading to host-guest inclusion complexes

Formations of host-guest inclusion complexes of two ionic liquids (namely, 1-butyl-3-methylimidazolium chloride and 1-butyl-1-methylpyrrolidinium chloride) with α and β-cyclodextrins have been investigated by physicochemical and spectroscopic methods as stabilizer, carrier and regulatory releaser of the guest molecules. ^{1}H NMR, 2D ROESY NMR, FT-IR and ESI MS studies confirm the inclusion phenomenon, whereas surface tension and conductivity studies recommend 1:1 stoichiometry of the inclusion complexes. The interactions of cyclodextrin with the above two ionic liquids were characterized by density, viscosity and refractive index measurements, while the binding constants have been evaluated using non-linear programme by conductivity method, indicating higher degree of encapsulation in case of α-cyclodextrin than that in β-cyclodextrin. The formations of inclusion complexes were elucidated by hydrophobic effect, structural effect, electrostatic force and H-bonding interactions.

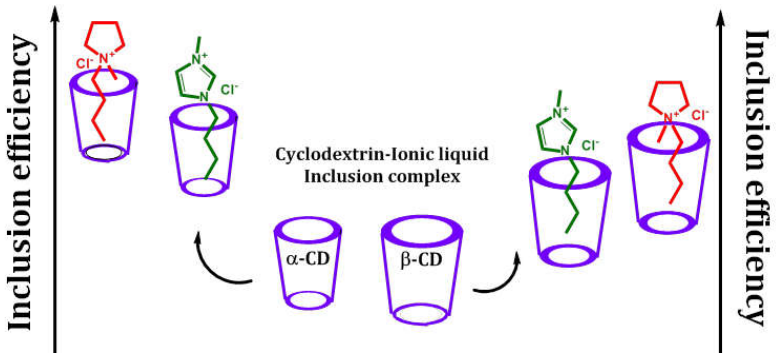

IX.1. Introduction

Cyclodextrins (CDs) are focused with great interests in the field of modern biochemistry since the discovery for their unique property for controlled release of enormous compounds due to formation of inclusion complex (IC) with hydrophobic guest molecules [1]. Thus, CDs have vast applications in various industries including pharmaceutical, food, textile, pesticides, cosmetic sectors etc [2]. CDs are cyclic oligomer of α-D-glucose having different number of glucopyranose units (6 for α-CD, 7 for β-CD & 8 for γ-CD) bound by α-(1-4) linkages [3]. They have a shape of truncated cone with a fairly rigid and well-defined hydrophobic cavity of varying diameter and two discrete rims, a wider rim having all secondary hydroxyl groups and a narrow rim having all primary hydroxyl groups (Scheme IX.1) [3]. Thus, the structure of CD affords a hollow cone shaped segment which is competent to form stable supramolecular host-guest inclusion complex with variety of molecules [4]. Macrocyclic CD molecule always draws the attention in this field of chemistry owing to their exceptional structure and potential applications in the invention of molecular switches, molecular machines, supramolecular polymers, etc [5]. Conjugation of CD with various nanopaticles improves the characteristics of the entity helping in molecular recognition for the host to function as nano-sensors, drug delivery tools and recycling extraction agents [6].

Ionic liquids (ILs) have vast applications in chemical reactions, synthesis, cellulose processing, nuclear fuel reprocessing, waste recycling, metal air batteries etc [7]. They are considered as green solvents as they do not produce any environmental hazards [8]. ILs have exceptional features such as low vapor pressure, thermal stability, solvating properties and wide liquid regions [7]. Because of their distinctive properties they are attracting increasing attention in many fields such as organic chemistry, electrochemistry, catalysis, physical chemistry and applied supramolecular chemistry [9-15]. In our previous works inclusion phenomenon of various ILs with CDs have been shown and characterized [16-18].

In this article the two studied ILs, namely, 1-butyl-3-methylimidazolium chloride [BMIm]Cl and 1-butyl-1-methylpyrolidinium chloride [BMP]Cl (Scheme IX.2) are currently of interest in industry owing to their ability to be infinitely recycled and their ready solvation at room temperature making them excellent green solvents [7]. CD-IL ICs have wide applications in industry for their stability against atmospheric hazards and long term uses without chemical modification. We investigated the formation of host-guest inclusion complexes (ICs) of these two ILs with α and β-CD particularly towards their formation, stabilization, carrying and controlled release without chemical modification by different dependable methods like ^{1}H NMR, 2D ROESY NMR, FT-IR, ESI MS, surface tension, conductivity, density, viscosity and refractive index measurements.

IX.2. Experimental section

IX.2.1. Source and purity of samples

The selected ionic liquids and cyclodextrins of puriss grade were bought from Sigma-Aldrich, Germany and used as purchased. The mass fraction purity of [BMIm]Cl, [BMP]Cl, *α*-cyclodextrin and *β*-cyclodextrin were ≥ 0.99, 0.99, 0.98 and 0.98 respectively.

IX.2.2. Apparatus and procedure

Solubilities of the two CDs and above mentioned two ionic liquids have been verified in triply distilled, deionized and degassed water. The two ionic liquids were fairly soluble in aqueous CDs. All the stock solutions of [BMIm]Cl and [BMP]Cl were prepared by mass (Mettler Toledo AG-285 with uncertainty 0.0001 g) and the working solutions were obtained by mass dilution at 298.15 K. Densities of the solutions were used to change molarity to molality [19].

^{1}H NMR and 2D ROESY NMR spectra were recorded in D_2O at 300 MHz using Bruker Avance 300 MHz instrument at 298.15K. Signals are cited as δ values in ppm using residual protonated solvent signals as internal standard (HDO δ = 4.79 ppm). Data are reported as chemical shift.

Surface tensions of the solutions were measured with the help of platinum ring detachment technique by a Tensiometer (K9, KRŰSS; Germany) at 298.15 K. (Accuracy ±0.1 mN m ^{1}.) Temperature of the system was maintained by circulating thermostated water through a double-wall glass vessel holding the solution.

Conductivities of the solutions were studied by Mettler Toledo Seven Multi conductivity meter having uncertainty 1.0 μSm^{-1}. The study was carried out in a thermostated water bath at 298.15K with uncertainty ±0.01K. HPLC grade water was used with specific conductance 6.0 μS m^{-1}. The conductivity cell was calibrated using 0.01M aqueous KCl solution.

The densities (ρ) of the solutions were studied by vibrating *U*-tube Anton Paar digital density meter (DMA 4500M) having precision ±0.00005 g cm^{-3} and uncertainty in temperature was ±0.01K. The density meter was calibrated by standard method [19].

Viscosities (η) were determined by Brookfield DV-III Ultra Programmable Rheometer with spindle size 42. The detail has already been depicted before [19].

Refractive indexes of the solutions were studied with a Digital Refractometer from Mettler Toledo having uncertainty ±0.0002 units. The detail has already been described before [19].

Each of the four solid inclusion complexes ([BMIm]Cl + α-CD, [BMP]Cl + α-CD, [BMIm]Cl + β-CD and [BMP]Cl + β-CD) has been prepared in 1:1 molar ratio of the ionic liquid and cyclodextrin. In each case 1.0 mmol cyclodextrin was dissolved in 20 mL water and 1.0 mmol ionic liquid was dissolved in 20 mL ethanol and stirred separately for 3 hrs. Then the ethanol solution of the ionic liquid was added drop by drop to the aqueous CD solution. The mixture was then allowed to stir for 48 hrs at 50–55^{o}C. It was filtered at this temperature, then cooled to 5^{o}C and kept for 12 hrs. The resulting suspension was filtered and the

white polycrystalline powder was found, which was washed with ethanol and dried in air.

HRMS analyses were executed with Q-TOF high resolution instrument by positive mode electro-spray ionization dissolving the solid ICs in methanol.

Fourier transform infrared (FT-IR) spectra were recorded on a Perkin Elmer FT-IR spectrometer according to the KBr disk technique. Samples were prepared as KBr disks with 1 mg complex and 100 mg KBr. The FTIR measurements were performed in the scanning range of 4000 400 cm ^{1} at room temperature.

IX.3. Results and discussion

IX.3.1. ^{1}H NMR study establishes inclusion

NMR study is the most important tool which ascertains the inclusion phenomena of the guest IL inside the host CD molecule. In this work we have studied the interactions of the two ILs (*viz.*, [BMIm]Cl and [BMP]Cl) with α and β-CD by ^{1}H NMR study taking 1:1 molar ratio of IL and CD in D_2O at 298.15K (Figure IX.1-IX.4). ^{1}H NMR data of the two ILs, two CDs and four ICs are listed in table IX.1. The protons of the CD molecule show considerable chemical shift due to the incorporation of guest IL into its hydrophobic cavity [20]. In the structure of CD, the H3 and H5 are situated inside the cavity, more precisely the position of H3 and H5 protons are near the wider rim and narrower rim respectively while the H1, H2 and H4 protons are found at the periphery of CD molecule (Scheme IX.3) [21-22]. During the insertion of guest IL molecule inside the cavity of CD, the H3 and H5 protons show upfield chemical shift as a result of interaction with the guest, which confirm the formation of host-guest inclusion complexes. The IL molecules insert into the host CD through the wider rim, as a result the H3 protons located near the wider rim show higher shift than the H5 protons which are present near the narrower rim at the interior of CD (Scheme IX.4). Upfield chemical shift is also observed for the exterior protons but to lesser extent. The interacting protons of the two studied ILs also show upfield chemical shift. The

shifts in butyl as well as methyl groups are found in case of [BMP]Cl, while only shift in butyl group is observed in case of [BMIm]Cl, which illustrates the mechanism of insertion as depicted in Scheme IX.5. Besides, the shifts of butyl protons in [BMP]Cl are more in comparison to that in [BMIm]Cl for both CDs, indicating binding affinity of the former is more compared to the latter.

IX.3.2. 2D ROESY NMR elucidates binding mode

2D ROESY NMR provides valuable information about the binding mode of the two ionic liquids [BMIm]Cl and [BMP]Cl with host CD molecules and also helpful to understand the geometry of the inclusion complexes, as any two protons that are closely located in space within a distance of 0.4 nm can produce a nuclear overhauser effect (NOE) cross co-relation in NOE spectroscopy (NOESY) or rotating-frame NOE spectroscopy (ROESY) [23-26]. 2D ROESY NMR have been done using the four solid ICs of the ILs and CDs. Part of the contour plot of the ROESY spectrum of the [BMIm]Cl+α-CD IC and [BMP]Cl+α-CD IC have been shown in figure IX.5 and IX.6, whereas the spectra of the two ILs with β-CD have been provided in figure IX.7 and IX.8. As mentioned above, the H3 and H5 protons of CD are located in the hydrophobic cavity whereas H1, H2 and H4 protons are placed outside (Scheme IX.3). In all the four figures IX.5, IX.6, IX.7 and IX.8, there are appreciable correlation between the H3 or H5 protons of CD and the methelene and methyl groups of butyl chains of the two ILs, confirming that the butyl chain in both the guest ILs inserted in the hydrophobic cavity of the host CD molecules. The H6 protons of α and β-CD remain unaffected after the inclusion phenomenon which again support that the guest IL molecules inserted from the wider rim of CDs [27].Thus, 2D ROESY NMR results are in good agreement with results obtained from ^{1}H NMR chemical shifts analysis.

IX.3.3. Surface tension study supports inclusion

Surface tension (γ) is another valuable parameter which also suggests the formation of inclusion complex of the two studied ionic liquids with both α and β-CD [28]. Addition of CD to pure water does not show any considerable change

to the surface tension of water which is an indication that both cyclodextrins are almost surface inactive compounds [29]. In the present study the γ of aqueous ionic liquids have been determined with increasing concentration of α and *β*-CD at 298.15K (Table IX.2-IX.5). The *γ* values substantially increase for both [BMIm]Cl and [BMP]Cl with addition of CDs probably due to the removal of surface active ionic liquid molecules from surface of the solution, i.e., the hydrophobic tail of ionic liquids enter into the hydrophobic cavity of α and β-CD forming the host guest inclusion complexes [30-31]. All the four curves show a single break point and after that point the *γ* value becomes approximately steady which confirms the formation of 1:1 inclusion complex (Figure IX.9 and IX.10). More break points in the surface tension curve would indicate the formation of inclusion complex with complex stoichiometry such as 1:2, 2:1, 2:2 etc (Scheme IX.6) [32-33]. The values of γ and corresponding concentration of CDs and ILs at each break have been listed in table IX.6. The breaks have been found in certain concentration of ILs and CDs where their concentration ratio in the solution was almost 1:1. Hence this study proves the formation of 1:1 inclusion complex. The γ value at the break point is little higher in case of α-CD than β-CD which might be due to the fact that former is a better host than the latter.

IX.3.4. Conductivity study informs inclusion

The conductivity (κ) study not only confirms the formation of host-guest inclusion complex but also gives the stoichiometry of the assembly [34-36]. We have measured the conductivity of the aqueous solution of studied two ionic liquids having initially 10mmolL^{-1} concentration with successive addition of α and β-CD at 298.15K (Table IX.2-IX.5). It has been found that the conductivity of both the ionic liquid decreases on a regular basis with increasing concentration of CDs (Figure IX.11 and IX.12). This observation is in agreement with the formation of inclusion complex. Insertion of the guest ionic liquid molecule inside the cavity of the CD molecule decreases the mobility of the former, thus the number of free ions per unit volume decreases, resulting the reduction of conductivity of the solution. The four curves (Figure IX.11 and IX.12) show

similar result, each having a noticeable break suggesting the formation of IL-CD inclusion complex having stoichiometry 1:1. The values of κ and corresponding concentration of the two ILs and CDs at each break point are listed in table IX. 7. In both the cases of [BMIm]Cl and [BMP]Cl the conductivity values at the break points are lower for α-CD than β-CD suggesting that the former is better to encapsulate the guests than the later.

IX.3.5. Density study: interaction between host and guest

Density study may be applied to obtain valuable information about the interaction (here inclusion) between ionic liquids and CD molecules. The two parameters used for this purpose are apparent molar volume (ϕ_v) and limiting apparent molar volume (ϕ_v^o) [28]. The sum of the geometric volume of the central solute molecule and changes in the solvent volume as a result of interaction with the solute around the co-sphere is termed as apparent molar volume [37]. Ionic liquid + aqueous CD is a ternary solution system. The limiting apparent molar volume is used to express solute-solvent interactions of this system (here, solute = IL and co-solvent = CD). For the present study ϕ_v have been measured from the solutions density at 298.15 K (table IX.10). ϕ_v^o were obtained by a least-square treatment to the plots of ϕ_v versus $\sqrt{m}$ using the Masson equation (Table VI.11) [38]. It is found that ϕ_v values regularly decrease and ϕ_v^o values constantly increase for the two studied IL with increasing concentration of both α and β-CD. Thus, it is evident that in both cases of [BMIm]Cl and [BMP]Cl the ion–hydrophilic group interactions are more effective than ion–hydrophobic group interactions. The ϕ_v^o values for both the ILs and CDs at different mass fractions are depicted in figure IX.13. The ϕ_v^o values are found to be more for [BMP]Cl than [BMIm]Cl due to higher interaction of the hydrophobic groups of the former than the letter within the cavity of CDs. The values of ϕ_v^o increases with increasing mass fractions of both CDs and also found grater for α-CD than β-CD, indicating the former interacts more with the ILs than the latter. This may be explained as in case of [BMP]Cl, both the butyl and methyl groups can be encapsulated into the cavity of CD and the single positively

charged N atom show higher ion-hydrophilic interaction with the –OH groups of CD. In case of [BMIm]Cl, only the butyl group can be encapsulated into the cavity of CD and the ion-hydrophilic interaction is less because of sharing of positive charge between two N atoms. The smaller diameter of α-CD helps in making more compact structure with the ILs than β-CD with relatively larger cavity size showing less hydrophobic interactions with ILs.

IX.3.6. Viscosity study: order of interactions

The interaction between ILs and CDs can also be interpreted using viscosity study [39]. The viscosity of the solutions show an increasing trend with increasing concentrations of both the ILs in the present ternary system (IL + aqueous CD), (Table IX.9). The viscosity *B*-coefficients (Table IX.11) signifies the solute–solvent interactions (here, solute = IL and co-solvent = CD) that depends upon the size and shape of the solute molecules. For the two ILs, *viz.*, [BMIm]Cl and [BMP]Cl, the viscosity *B*-coefficients are depicted in Figure IX.14 and found to be all positive. It may be observed that the viscosity *B* values increase with increasing concentration of CDs probably due to greater IL-CD interaction and also higher salvation [30]. It is again greater for α-CD than β-CD for the two ILs suggesting that inclusion is more favorable in case of former than the latter. The comparative result of [BMIm]Cl and [BMP]Cl for viscosity *B*-coefficient has been found similar as for the density study, thus it is the structural feature of the two ILs and CDs as explained earlier for which these trends of interactions have been obtained.

IX.3.7. Refractive index shows the compactness of the inclusion complexes

Refractive index is another valuable parameter to establish the molecular interaction in the above mentioned ternary solution systems [28]. The refractive index (n_D) and molar refraction (R_M) values of the solutions have been estimated using suitable equation (Table IX.9 and IX.10). Greater values of R_M and the limiting molar refraction (R^0_M) signify that the medium is more compact and dense (Table IX.11) [29, 30]. Here the R^0_M values show an increasing trend with

increasing concentrations of both CDs, suggesting that the IC of [BMP]Cl with both α and β-CD are more closely packed than those of [BMIm]Cl perhaps due to greater hydrophobic as well as ion-hydrophilic interactions between the guest and host as described earlier. The R^0_M values indicate that α-CD is more efficient than β-CD in forming the ICs (FigureIX.15). The observations obtained from refractive index data are in agreement with the density and viscosity studies.

IX.3.8. Binding constants: non-linear isotherms by conductivity method

Binding constants (K_b) for the inclusion process have been determined for the four IL-CD ICs with the help of conductivity study. Here, non-linear programme has been used basing upon the changes in conductivity as a result of encapsulation of the IL molecule inside into the apolar cavity of α and β-CD [40, 41]. The following equilibrium is supposed to exist between the host and the guest for 1:1 IC

$$IL_f + CD_f \overset{K_b}{\rightleftharpoons} IC \qquad (1)$$

The binding constant (K_b) for the formation of IC may be expressed as

$$K_b = \frac{[IC]}{[IL]_f[CD]_f} \qquad (2)$$

Here, [IC], $[IL]_f$ and $[CD]_f$ represent the equilibrium concentration of IC, free IL molecule and free CD respectively. According to the binding isotherm, the binding constant (K_b) for the formation of IC may be expressed as

$$K_b = \frac{[IC]}{[IL]_f[CD]_f} = \frac{(\kappa_{obs}-\kappa_o)}{(\kappa-\kappa_{obs})[CD]_f} \qquad (3)$$

where, $$[CD]_f = [CD]_{ad} \quad \frac{[IL]_{ad}(\kappa_{obs}-\kappa_o)}{(\kappa-\kappa_o)} \qquad (4)$$

Here, κ_o, κ_{obs} and κ are the conductivity of IL molecule at initial state, during addition of CD and final state respectively. $[IL]_{ad}$ and $[CD]_{ad}$ are the concentrations of IL and the added CD respectively. Thus, the values of K_b for the ICs were evaluated from the binding isotherm by applying non-linear

programme (Table IX.12) [42] which indicate that [BMP]Cl has higher binding constant than [BMIm]Cl for ICs with both CDs, while, α-CD encapsulates both ILs more tightly than β-CD does, may be because of narrower cavity dimension of α-CD, which structurally fits better than β-CD with the ILs investigated in this work.

IX.3.9. ESI-mass spectrometric analysis of inclusion complexes

ESI-mass spectrometric analyses were carried out for the four solid ICs synthesized by the method described in experimental procedure section and have been shown in figure IX.16 and IX.17. The observed peaks have been put into table IX. 13, which confirm that in all cases the desired ICs have been formed in solid state and the stoichiometric ratio of the host and guest is 1:1 [43, 44].

IX.3.10. FT-IR Spectra of solid inclusion complexes

FT-IR spectrum also proves the inclusion phenomena in solid state [45-47]. The characteristic IR frequencies of [BMIm]Cl, [BMP]Cl, α-CD, β-CD and solid ICs are listed in table IX.14. The FT-IR Spectra of [BMIm]Cl is characterized by presence of peaks for -C=N,-C-N, -C=C etc. bonds, whereas [BMP]Cl is characterized with peaks for -C-N and -C-H for $-CH_3$ and CH_2 groups (Figure IX.18-IX.19 and IX.20-IX.21). Broad characteristic peaks of –OH at about 3412.10 cm^{-1} and 3349.84 cm^{-1} are present in the spectrum for α and β-CD. However, several peaks of the two ILs are either absent or shifted which is due to the change in environment of the two guests after inclusion in the cavity of CDs. The –C-H stretching bands for $-CH_3$ and $-CH_2$ of both the ILs are absent in the inclusion spectrum. The –O-H stretching of both α and β-CD is shifted to lower frequency in the spectrum of four ICs possibly due to involvement of the –O-H groups of the host molecules in hydrogen bonding with the guest molecules. The peaks for the C-N group of the guest molecules are present in the spectrum of the ICs, which is an indication of the fact that the hydrophobic side chains of both the IL molecules are encapsulated in the hydrophobic cavity of α and β-CD.

IX.3.11. Structural influence of cyclodextrin

The formation of host-guest ICs between the two studied ILs and CDs not only depends upon the size of the guest molecules but also on the cavity diameter of host. The cavity diameter of α and β-CD are 4.7-5.3 Å and 6.0-6.5Å respectively. Considering the size of the two ILs (overall length of [BMIm]Cl is 5.29 Å, [BMP]Cl is 4.62 Å, but the length of inserted butyl chain is 3.08 Å), it is found that α-CD is more suitable for forming ICs with both ILs perhaps due to more surface interaction, increasing the hydrophobic attractions, which is in agreement with spectroscopic and physicochemical observations [1]. The hydrophobic butyl chains of both the ILs are encapsulated into the hydrophobic cavity of CD molecules and no covalent bonds are formed or broken during the formation of ICs. One of the main factors for the formation of IC is that the hydrophobic cavity of CD is occupied by polar water molecule which is unfavourable, so the water molecules are easily substituted by more hydrophobic tails of IL and the trapped water molecules are released in bulk of the solution which increases the entropy of the system [48-50]. It results in a more stable lower energy state of the system and also reduces the ring strain of CD moiety [48-49]. The stiochiometry of the host-guest IC is 1:1 probably because of difficulty for the second molecule of IL to be trapped by the cavity after inclusion of one. The N atoms of the two ILs form H-bonds with the –OH groups at the rim of CD, thus stabilizing the whole IC.

IX.4. Conclusion

With the help of the above mentioned spectroscopic and physicochemical studies we reach to the conclusion that the two ILs, *viz.*, [BMIm]Cl and [BMP]Cl form host-guest ICs with both α and β-CD both in solution and solid state. ^{1}H NMR and 2D ROESY NMR data confirm the inclusion in the apolar cavity of both CD molecules, while surface tension and conductivity measurement suggest 1:1 stoichiometry. Density, viscosity and refractive index data are also in good agreement with the above results and also recommend the IL-CD interactions.

Binding constants for the ICs have been determined with the help of conductivity study by using non-linear programme. The solid state characterisations have been done by ESI-MS and FT-IR, confirming their formations also in solid state. The inclusion phenomenon has been found more fascinated in case of α-CD and [BMP]Cl than the other combinations. Thus, the present study has miscellaneous application in the field of nano-sensors, drug delivery tools and recycling extraction agents etc.

Published in RSC Advances, 2016, 6, 100016 – 100027

Tables:

Table IX.1. ^{1}H NMR data of [BMIm]Cl, [BMP]Cl, α-CD, β-CD and inclusion complexes

[BMIm]Cl (300MHz, Solv: D_2O) δ /ppm	[BMP]Cl (300MHz, Solv: D_2O) δ /ppm
0.87-0.92 (3H, t, *J* = 7.26 Hz), 1.26-1.33(2H, m), 1.78-1.85 (2H, m), 3.87 (3H, s), 4.15-4.20 (2H, t, *J* = 7.11 Hz), 7.40 (1H, s), 7.45 (1H, s), 8.69 (1H, s)	0.91-0.96 (3H, t, *J* = 7.29 Hz), 1.34-1.41 (2H, m), 1.74-1.81(2H,m), 2.19 (4H, m), 3.02 (3H, s), 3.28-3.34 (2H, m), 3.48 (4H, m)
α-Cyclodextrin (500 MHz, Solv: D_2O) δ /ppm	β-Cyclodextrin (400 MHz, Solv: D_2O) δ /ppm
3.48-3.51 (6H, t, *J*= 9.00 Hz), 3.53-3.56 (6H, dd, *J*= 10.00, 3.00 Hz), 3.74-3.83 (18H, m), 3.87-3.91 (6H, t, *J* = 9 Hz), 4.96-4.97 (6H, d, *J* = 3 Hz)	3.49-3.54 (6H, t, *J* = 9.2 Hz), 3.57-3.60 (6H, dd, *J* = 9.6, 3.2 Hz), 3.79-3.84 (18H, m), 3.87-3.92 (6H,t, *J* = 9.2 Hz), 5.00-5.01 (6H, d, *J* = 3.6 Hz)
[BMIm]Cl-α-CD (1:1 molar ratio, 300 MHz, Solv: D_2O) δ /ppm	[BMP]Cl- α-CD (1:1 molar ratio, 300 MHz, Solv: D_2O) δ /ppm
0.84-0.89 (3H, t, *J* = 7.26 Hz), 1.22-1.29 (2H, m), 1.74-1.81 (2H, m), 3.48-3.51 (6H, t, *J*= 9.00 Hz), 3.53-3.56 (6H, dd, *J*= 10.00, 3.00 Hz), 3.71-3.79 (18H, m), 3.80-3.83 (6H, t, *J* = 9 Hz), 3.84 (3H, s), 4.11-4.16 (2H, t, *J* = 7.11 Hz), 4.96-4.97 (6H, d, *J* = 3 Hz), 7.40 (1H, s), 7.45 (1H, s), 8.69 (1H, s)	0.88-0.93 (3H, t, *J* = 7.29 Hz), 1.31-1.38 (2H, m), 1.71-1.78 (2H,m), 2.19 (4H, m), 3.00 (3H, s), 3.25-3.31 (2H, m), 3.48 (4H, m), 3.49-3.51 (6H, t, *J*= 9.00 Hz), 3.53-3.56 (6H, dd, *J*= 10.00, 3.00 Hz), 3.80-3.85 (18H, m), 3.88-3.93 (6H, t, *J* = 9 Hz), 4.96-4.97 (6H, d, *J* = 3 Hz)
[BMIm]Cl-β-CD (1:1 molar ratio, 300 MHz, Solv: D_2O) δ /ppm	[BMP]Cl- β-CD (1:1 molar ratio, 300 MHz, Solv: D_2O) δ /ppm
0.85-0.90 (3H, t, *J* = 7.26 Hz), 1.23-1.30 (2H, m), 1.75-1.82 (2H, m), 3.49-3.54 (6H, t, *J* = 9.2 Hz), 3.57-3.60 (6H, dd, *J* = 9.6, 3.2 Hz), 3.72-3.80 (18H, m), 3.81-3.84 (6H,t, *J* = 9.2 Hz), 3.85 (3H, s), 4.12-4.17 (2H, t, *J* = 7.11 Hz), 5.00-5.01 (6H, d, *J* = 3.6 Hz), 7.40 (1H, s), 7.45 (1H, s), 8.69 (1H, s)	0.89-0.94 (3H, t, *J* = 7.29 Hz), 1.32-1.40 (2H, m), 1.72-1.79 (2H,m), 2.19 (4H, m), 3.03 (3H, s), 3.27-3.34 (2H, m), 3.48 (4H, m), 3.49-3.51 (6H, t, *J*= 9.00 Hz), 3.53-3.56 (6H, dd, *J*= 10.00, 3.00 Hz), 3.82-3.87 (18H, m), 3.89-3.95 (6H, t, *J* = 9 Hz), 4.96-4.97 (6H, d, *J* = 3 Hz)

Table IX.2. Data for surface tension and conductivity study of aqueous [BMIm]Cl-*α*-CD system at 298.15K[a]

Volm of *α*-CD (mL)	Total volm (mL)	Conc of [BMIm]Cl (mM)	Conc of *α*-CD (mM)	Surface tension (mN m^{-1})	Conductuvity (mS m^{-1})
0	10	10.000	0.000	42.0	4.52
1	11	9.091	0.909	45.9	4.14
2	12	8.333	1.667	49.8	3.85
3	13	7.692	2.308	53.3	3.57
4	14	7.143	2.857	56.3	3.36
5	15	6.667	3.333	58.8	3.18
6	16	6.250	3.750	61.1	2.98
7	17	5.882	4.118	63.3	2.84
8	18	5.556	4.444	64.9	2.70
9	19	5.263	4.737	66.8	2.57
10	20	5.000	5.000	68.7	2.42
11	21	4.762	5.238	69.0	2.39
12	22	4.545	5.455	69.2	2.36
13	23	4.348	5.652	69.3	2.34
14	24	4.167	5.833	69.4	2.32
15	25	4.000	6.000	69.5	2.30
16	26	3.846	6.154	69.6	2.28
17	27	3.704	6.296	69.7	2.26
18	28	3.571	6.429	69.8	2.24
19	29	3.448	6.552	69.9	2.22
20	30	3.333	6.667	70.0	2.20

[a] Standard uncertainties in temperature *u* are: *u*(T) = ±0.01 K.

Table IX.3. Data for surface tension and conductivity of aqueous [BMIm]Cl-*β*-CD system at 298.15K[a]

Volm of *β*-CD (mL)	Total volm (mL)	Conc of [BMIm]Cl (mM)	Conc of *β*-CD (mM)	Surface tension (mN m^{-1})	Conductuvity (mS m^{-1})
0	10	10.000	0.000	42.0	4.58
1	11	9.091	0.909	46.3	4.21
2	12	8.333	1.667	50.3	3.93
3	13	7.692	2.308	53.5	3.70
4	14	7.143	2.857	56.6	3.48
5	15	6.667	3.333	58.9	3.29
6	16	6.250	3.750	61.2	3.13
7	17	5.882	4.118	63.0	2.99
8	18	5.556	4.444	64.7	2.86
9	19	5.263	4.737	66.5	2.75
10	20	5.000	5.000	68.1	2.62
11	21	4.762	5.238	68.4	2.59
12	22	4.545	5.455	68.8	2.56
13	23	4.348	5.652	69.2	2.54
14	24	4.167	5.833	69.5	2.52
15	25	4.000	6.000	69.7	2.50
16	26	3.846	6.154	69.9	2.48
17	27	3.704	6.296	70.1	2.46
18	28	3.571	6.429	70.3	2.44
19	29	3.448	6.552	70.5	2.42
20	30	3.333	6.667	70.7	2.40

[a] Standard uncertainties in temperature *u* are: *u*(T) = ±0.01 K.

Table IX.4. Data for surface tension and conductivity study of aqueous [BMP]Cl-α-CD system at 298.15K[a]

Volm of α-CD (mL)	Total volm (mL)	Conc of [BMP]Cl (mM)	Conc of α-CD (mM)	Surface tension (mN m^{-1})	Conductuvity (mS m^{-1})
0	10	10.000	0.000	39.0	5.00
1	11	9.091	0.909	42.9	4.59
2	12	8.333	1.667	47.2	4.25
3	13	7.692	2.308	50.9	3.99
4	14	7.143	2.857	54.0	3.76
5	15	6.667	3.333	56.8	3.55
6	16	6.250	3.750	59.4	3.38
7	17	5.882	4.118	61.6	3.21
8	18	5.556	4.444	63.7	3.08
9	19	5.263	4.737	65.7	2.95
10	20	5.000	5.000	67.6	2.80
11	21	4.762	5.238	67.8	2.77
12	22	4.545	5.455	68.0	2.74
13	23	4.348	5.652	68.2	2.71
14	24	4.167	5.833	68.4	2.68
15	25	4.000	6.000	68.5	2.65
16	26	3.846	6.154	68.6	2.62
17	27	3.704	6.296	68.7	2.59
18	28	3.571	6.429	68.8	2.56
19	29	3.448	6.552	68.9	2.53
20	30	3.333	6.667	69.0	2.50

[a] Standard uncertainties in temperature u are: u(T) = ±0.01 K.

Table IX.5. Data for surface tension and conductivity study of aqueous [BMP]Cl-*β*-CD system at 298.15K[a]

Volm of *β*-CD (mL)	Total volm (mL)	Conc of [BMP]Cl (mM)	Conc of *β*-CD (mM)	Surface tension (mN m^{-1})	Conductuvity (mS m^{-1})
0	10	10.000	0.000	39.0	5.21
1	11	9.091	0.909	43.2	4.82
2	12	8.333	1.667	47.5	4.47
3	13	7.692	2.308	51.0	4.21
4	14	7.143	2.857	53.9	3.95
5	15	6.667	3.333	56.7	3.73
6	16	6.250	3.750	59.1	3.53
7	17	5.882	4.118	61.3	3.37
8	18	5.556	4.444	63.3	3.22
9	19	5.263	4.737	65.0	3.09
10	20	5.000	5.000	66.9	2.98
11	21	4.762	5.238	67.4	2.94
12	22	4.545	5.455	67.8	2.90
13	23	4.348	5.652	68.1	2.87
14	24	4.167	5.833	68.4	2.84
15	25	4.000	6.000	68.7	2.81
16	26	3.846	6.154	69.0	2.79
17	27	3.704	6.296	69.3	2.77
18	28	3.571	6.429	69.6	2.75
19	29	3.448	6.552	69.8	2.73
20	30	3.333	6.667	70.0	2.71

[a] Standard uncertainties in temperature *u* are: *u*(T) = ±0.01 K.

Table IX.6. Values of surface tension (γ) at the break point with corresponding concentrations of cyclodextrins and ionic liquids at 298.15 K [a]

	Conc of α-CD /mM	Conc of ionic liquid /mM	γ [a] /mN·m^{-1}
[BMIm]Cl	5.17	4.83	68.91
[BMP]Cl	5.15	4.85	67.75
	Conc of β-CD /mM	Conc of ionic liquid /mM	γ [a] /mN·m^{-1}
[BMIm]Cl	5.10	4.90	68.26
[BMP]Cl	5.16	4.84	67.19

[a] Standard uncertainties (u): temperature: u(T) = ±0.01 K, surface tension: $u(\gamma)$ = ±0.1 mN m ^{1}

Table IX.7. Values of conductivity (κ) at the break point with corresponding concentrations of cyclodextrins and ionic liquids at 298.15 K [a]

	Conc of α-CD /mM	Conc of ionic liquid /mM	κ [a] /mS·m^{-1}
[BMIm]Cl	5.14	4.86	2.41
[BMP]Cl	5.03	4.97	2.82
	Conc of β-CD /mM	Conc of ionic liquid /mM	κ [a] /mS·m^{-1}
[BMIm]Cl	5.07	4.93	2.62
[BMP]Cl	5.01	4.99	2.97

[a] Standard uncertainties (u): temperature: u(T) = ±0.01 K, conductivity: $u(\kappa)$ = ±1.0 μS·m^{-1}.

Table IX.8. Experimental values of density (ρ), viscosity (η) and refractive index (n_D) of different mass fractions of aqueous α and β-cyclodextrin mixtures at 298.15 K[a]

Aqueous solvent mixture	$\rho\times10^{-3}$ /kg m^{-3}	η /mP s	n_D
aq. α-CD			
w_1 = 0.001	0.99735	1.29	1.3329
w_1 = 0.003	0.99802	1.30	1.3332
w_1 = 0.005	0.99868	1.31	1.3335
aq. β-CD			
w_2 = 0.001	0.99755	1.30	1.3328
w_2 = 0.003	0.99819	1.31	1.3331
w_2 = 0.005	0.99895	1.32	1.3334

[a] Standard uncertainties u are: $u(\rho)$ = 5×10^{-5} g cm^{-3}, $u(\eta)$ = 0.003 mP s, $u(n_D)$ =0.0002, and u(T) = ±0.01K.

Table IX.9. Experimental values of density (ρ), viscosity (η) and refractive index (nD) of selected ionic liquids in different mass fractions of aqueous α and β-cyclodextrin mixtures at 298.15 K[a]

molality /mol kg^{-1}	$\rho\times10^{-3}$ /kg m^{-3}	η /mP s	n_D	molality /mol kg^{-1}	$\rho\times10^{-3}$ /kg m^{-3}	η /mP s	n_D
[BMIm]Cl							
w_1 = 0.001[b]				w_2 = 0.001[b]			
0.010034	0.99836	1.36	1.3330	0.010032	0.99858	1.38	1.3330
0.025113	0.99988	1.41	1.3331	0.025106	1.00014	1.43	1.3331
0.040225	1.00140	1.44	1.3332	0.040212	1.00171	1.47	1.3333
0.055370	1.00293	1.47	1.3333	0.055350	1.00329	1.49	1.3334
0.070548	1.00446	1.50	1.3334	0.070518	1.00488	1.53	1.3336
0.085760	1.00599	1.52	1.3335	0.085717	1.00648	1.56	1.3338
w_1 = 0.003[b]				w_2 = 0.003[b]			
0.010027	0.99901	1.39	1.3334	0.010025	0.99924	1.40	1.3334
0.025096	1.00053	1.45	1.3335	0.025088	1.00087	1.46	1.3335

0.040198	1.00207	1.49	1.3336	0.040178	1.00255	1.50	1.3337
0.055332	1.00361	1.54	1.3337	0.055295	1.00428	1.54	1.3339
0.070497	1.00517	1.56	1.3338	0.070432	1.00610	1.57	1.3341
0.085695	1.00674	1.59	1.3339	0.085595	1.00789	1.60	1.3343
w_1 = 0.005[b]				w_2 = 0.005[b]			
0.010021	0.99962	1.41	1.3339	0.010018	0.99999	1.42	1.3336
0.025083	1.00105	1.48	1.3340	0.025066	1.00173	1.49	1.3337
0.040181	1.00249	1.53	1.3341	0.040138	1.00355	1.54	1.3338
0.055311	1.00398	1.57	1.3342	0.055227	1.00549	1.57	1.3340
0.070475	1.00548	1.60	1.3343	0.070333	1.00749	1.61	1.3342
0.085671	1.00702	1.64	1.3344	0.085459	1.00948	1.65	1.3343
[BMP]Cl							
w_1 = 0.001[b]				w_2 = 0.001[b]			
0.010035	0.99832	1.37	1.3347	0.010032	0.99855	1.39	1.3345
0.025116	0.99983	1.42	1.3348	0.025110	1.00008	1.45	1.3346
0.040233	1.00130	1.46	1.3349	0.040220	1.00163	1.49	1.3347
0.055383	1.00282	1.50	1.3350	0.055364	1.00320	1.53	1.3348
0.070570	1.00433	1.52	1.3351	0.070540	1.00479	1.56	1.3349
0.085792	1.00583	1.55	1.3352	0.085746	1.00641	1.59	1.3350
w_1 = 0.003[b]				w_2 = 0.003[b]			
0.010028	0.99894	1.39	1.3352	0.010025	0.99924	1.41	1.3346
0.025103	1.00034	1.45	1.3353	0.025088	1.00092	1.47	1.3347
0.040215	1.00175	1.50	1.3354	0.040178	1.00269	1.52	1.3348
0.055363	1.00318	1.53	1.3355	0.055285	1.00461	1.55	1.3349
0.070550	1.00461	1.56	1.3356	0.070408	1.00665	1.60	1.3350
0.085770	1.00608	1.60	1.3357	0.085544	1.00875	1.63	1.3352
w_1 = 0.005[b]				w_2 = 0.005[b]			
0.010022	0.99955	1.41	1.3357	0.010018	0.99993	1.43	1.3350
0.025089	1.00087	1.47	1.3358	0.025072	1.00157	1.50	1.3351
0.040196	1.00221	1.52	1.3359	0.040151	1.00332	1.55	1.3352
0.055342	1.00357	1.55	1.3360	0.055252	1.00518	1.60	1.3353
0.070526	1.00494	1.60	1.3361	0.070372	1.00711	1.64	1.3354
0.085747	1.00635	1.64	1.3362	0.085500	1.00921	1.67	1.3355

[a] Standard uncertainties u are: $u(\rho)$ = 5×10^{-5} kg m^{-3}, $u(\eta)$ =0.003 mP s, $u(n_D)$ =0.0002, u(pH) =0.01 and u(T) =0.01K.

[b] w_1 and w_2 are mass fractions of α and β-cyclodextrin in aqueous mixture respectively.

Table IX.10. Apparent molar volume (ϕ_V), $(\eta_r\text{-}1)/\sqrt{m}$ and molar refraction (R_M) of selected ionic liquids in different mass fractions of aqueous α and β-cyclodextrin mixtures at 298.15 K[a]

molality /mol kg^{-1}	$\phi_V \times 10^6$ / m^3 mol^{-1}	$(\eta_r\text{-}1)/\sqrt{m}$ /kg$^{1/2}$mol$^{-1/2}$	$R_M \times 10^6$ /m^3 mol^{-1}	molality /mol kg^{-1}	$\phi_V \times 10^6$ / m^3 mol^{-1}	$(\eta_r\text{-}1)/\sqrt{m}$ /kg$^{1/2}$mol$^{-1/2}$	$R_M \times 10^6$ /m^3 mol^{-1}
[BMIm]Cl							
w_1 = 0.001[b]				w_2 = 0.001[b]			
0.010034	73.87	0.542	35.9878	0.010032	71.85	0.614	35.9799
0.025113	73.67	0.587	35.9429	0.025106	71.24	0.631	35.9336
0.040225	73.62	0.580	35.8982	0.040212	70.84	0.652	35.8968
0.055370	73.41	0.593	35.8532	0.055350	70.48	0.621	35.8501
0.070548	73.29	0.613	35.8083	0.070518	70.13	0.666	35.8128
0.085760	73.22	0.609	35.7636	0.085717	69.78	0.683	35.7753
w_1 = 0.003[b]				w_2 = 0.003[b]			
0.010027	75.82	0.691	36.0036	0.010025	69.80	0.686	35.9954
0.025096	74.42	0.728	35.9587	0.025088	67.59	0.723	35.9465
0.040198	73.57	0.729	35.9132	0.040178	65.79	0.724	35.9058
0.055332	73.18	0.785	35.8679	0.055295	64.06	0.747	35.8634
0.070497	72.67	0.753	35.8220	0.070432	61.78	0.748	35.8180
0.085695	72.22	0.762	35.7758	0.085595	60.66	0.757	35.7738
w_1 = 0.005[b]				w_2 = 0.005[b]			
0.010021	80.78	0.763	36.0306	0.010018	70.74	0.757	35.9879
0.025083	79.98	0.819	35.9889	0.025066	63.54	0.813	35.9352
0.040181	79.52	0.838	35.9470	0.040138	59.73	0.832	35.8798
0.055311	78.41	0.844	35.9034	0.055227	55.82	0.806	35.8300
0.070475	77.63	0.834	35.8596	0.070333	52.73	0.828	35.7783
0.085671	76.65	0.861	35.8145	0.085459	50.84	0.855	35.7175
[BMP]Cl							
w_1 = 0.001[b]				w_2 = 0.001[b]			
0.010035	80.38	0.619	36.6735	0.010032	77.90	0.691	36.6451
0.025116	78.18	0.636	36.6280	0.025110	76.70	0.728	36.5990
0.040233	78.63	0.657	36.5841	0.040220	75.90	0.729	36.5523
0.055383	77.92	0.692	36.5386	0.055364	75.17	0.752	36.5049
0.070570	77.66	0.671	36.4935	0.070540	74.46	0.753	36.4571
0.085792	77.61	0.688	36.4489	0.085746	73.66	0.762	36.4082
w_1 = 0.003[b]				w_2 = 0.003[b]			
0.010028	85.34	0.691	36.7003	0.010025	72.84	0.762	36.6298
0.025103	84.54	0.728	36.6589	0.025088	68.63	0.771	36.5782
0.040215	84.09	0.767	36.6172	0.040178	65.33	0.800	36.5235
0.055363	83.52	0.752	36.5749	0.055285	61.09	0.779	36.4636
0.070550	83.19	0.753	36.5327	0.070408	56.96	0.834	36.3996
0.085770	82.51	0.788	36.4892	0.085544	53.57	0.835	36.3434
w_1 = 0.005[b]				w_2 = 0.005[b]			
0.010022	90.29	0.763	36.7276	0.010018	79.25	0.833	36.6442
0.025089	89.69	0.771	36.6890	0.025072	72.45	0.861	36.5941

0.040196	89.04	0.800	36.6499	0.040151	67.99	0.870	36.5401
0.055342	88.38	0.779	36.6101	0.055252	63.96	0.902	36.4824
0.070526	87.86	0.834	36.5700	0.070372	60.66	0.914	36.4223
0.085747	87.05	0.860	36.5286	0.085500	56.52	0.907	36.3564

[a] Standard uncertainties u are: u(T) =0.01K.

[b] w_1 and w_2 are mass fractions of α and β-cyclodextrin in aqueous mixture respectively.

Table IX.11. Limiting apparent molar volume (ϕ_V^o), experimental slope (S_V*), viscosity A and B-coefficient and limiting molar refraction (R_M^o) of ionic liquids in different mass fractions of aqueous α and β-cyclodextrin mixtures at 298.15 K[a]

Aq. solvent mixture	$\phi^0_V \times 10^6$ / $m^3\ mol^{-1}$	$S^*_V \times 10^6$ /$m^3 mol^{-3/2} kg^{1/2}$	B /kg mol^{-1}	A /$kg^{1/2}\ mol^{-1/2}$	$R_M^0 \times 10^6$ /$m^3\ mol^{-1}$
		[BMIm]Cl			
w_1 = 0.001[b]	74.22	-3.423	0.332	0.517	36.12
w_1 = 0.003[b]	77.44	-18.18	0.384	0.661	36.14
w_1 = 0.005[b]	83.24	-21.15	0.431	0.736	36.16
		[BMP]Cl			
w_1 = 0.001[b]	81.08	-12.87	0.374	0.582	36.80
w_1 = 0.003[b]	86.8	-14.06	0.422	0.658	36.82
w_1 = 0.005[b]	92.17	-16.54	0.470	0.702	36.84
		[BMIm]Cl			
w_2 = 0.001[b]	72.93	-10.58	0.305	0.581	36.10
w_2 = 0.003[b]	75.06	-48.50	0.349	0.657	36.12
w_2 = 0.005[b]	80.6	-104	0.4	0.731	36.14
		[BMP]Cl			
w_2 = 0.001[b]	80.12	-21.54	0.349	0.662	36.78
w_2 = 0.003[b]	84.12	-100.8	0.390	0.715	36.80
w_2 = 0.005[b]	90.95	-115.7	0.432	0.79	36.82

[a] Standard uncertainties u are: u(T) =0.01K.

[b] w_1 and w_2 are mass fractions of α and β-cyclodextrin in aqueous mixture respectively.

Table IX.12. Binding constant (K_b) of various ionic liquid-cyclodextrin inclusion complexes

Temperature /K[a]	Binding constant $K_b \times 10^{-3}$ /M^{-1}[b]			
	[BMIm]Cl-α-CD	[BMP]Cl-α-CD	[BMIm]Cl-β-CD	[BMP]Cl-β-CD
293.15	2.07	2.39	1.95	2.19
298.15	1.94	2.23	1.81	2.06
303.15	1.79	2.02	1.65	1.93

[a] Standard uncertainties in temperature *u* are: *u*(T) = ±0.01 K.
[b] Mean errors in K_b = ±0.01×10^{-3} M^{-1}

Table IX.13. The observed peaks at different m/z with corresponding ions for the solid inclusion complexes

[BMIm]Cl-α-CD inclusion complex		[BMP]Cl-α-CD inclusion complex	
m/z	Ion	m/z	Ion
175.10	[BMImCl+H]+	178.14	[BMPCl+H]+
197.08	[BMImCl+Na]+	200.12	[BMPCl+Na]+
995.31	[α-CD+Na]+	995.31	[α-CD+Na]+
1147.42	[BMImCl+α-CD+H]+	1150.45	[BMPCl+α-CD+H]+
1169.40	[BMImCl+α-CD+Na]+	1172.44	[BMPCl+α-CD+Na]+
[BMIm]Cl-β-CD inclusion complex		[BMP]Cl-β-CD inclusion complex	
m/z	Ion	m/z	Ion
175.10	[BMImCl+H]+	178.14	[BMPCl+H]+
197.08	[BMImCl+Na]+	200.12	[BMPCl+Na]+
1157.36	[β-CD+Na]+	1157.36	[β-CD+Na]+
1309.47	[BMImCl+β-CD+H]+	1312.51	[BMPCl+β-CD+H]+
1331.45	[BMImCl+β-CD+Na]+	1334.49	[BMPCl+β-CD+Na]+

Table IX.14. Frequencies at FTIR spectra of [BMIm]Cl, [BMP]Cl, α-CD, β-CD and solid inclusion complexes

[BMIm]Cl		[BMP]Cl	
wave number / cm^{-1}	group	wave number / cm^{-1}	group
3436.81	=C-H	3409.96	–C-H from ring
2963.45	–C-H from $–CH_3$	2970.44	–C-H from $–CH_3$
1634.59	–C=N	1465.54	bending of –C-H from $–CH_2$
1574.80	C=C	1400.30	bending of –C-H from $–CH_3$
1464.89	bending $–CH_2$	1166.82	-C-N
1400.30	bending $–CH_2$		
1168.58	-C-N		
α-Cyclodextrin		β-Cyclodextrin	
wave number / cm^{-1}	group	wave number / cm^{-1}	group
3412.10	stretching of O-H	3349.84	stretching of O-H
2930.79	stretching of –C-H from $–CH_2$	2921.52	stretching of –C-H from $–CH_2$
1406.76	bending of –C-H from $–CH_2$ and bending of O-H	1412.36	bending of –C-H from $–CH_2$ and bending of O-H
1154.39	bending of C-O-C	1157.57	bending of C-O-C
1030.39	stretching of C-C-O	1033.51	stretching of C-C-O
952.36	skeletal vibration involving α-1,4linkage	938.53	skeletal vibration involving α-1,4linkage
[BMIm]Cl-α-CD inclusion complex		[BMP]Cl-α-CD inclusion complex	
wave number / cm^{-1}	group	wave number / cm^{-1}	group
3370.61	stretching of O-H of α-CD	3362.56	stretching of O-H of α-CD

2931.03	stretching of –C-H from –CH_2 of α-CD	2955.06	stretching of –C-H from –CH_2 of α-CD
1630.02	stretching of –C=N	1401.22	bending of –C-H from –CH_2 and bending of O-H of α-CD
1410.13	bending of –C-H from –CH_2 and bending of O-H of α-CD	1149.61	bending of C-O-C α-CD
1150.07	bending of C-O-C of α-CD	946.52	skeletal vibration involving α-1,4linkage
948.07	skeletal vibration involving α-1,4linkage		

[BMIm]Cl-β-CD inclusion complex		[BMP]Cl-β-CD inclusion complex	
wave number / cm^{-1}	group	wave number / cm^{-1}	group
3364.47	stretching of O-H Of β-CD	3369.85	stretching of O-H of β-CD
2932.46	stretching of –C-H from –CH_2 Of β-CD	2931.03	stretching of –C-H from –CH_2 Of β-CD
1407.57	bending of –C-H from –CH_2 and bending of O-H of β-CD	1408.47	bending of –C-H from –CH_2 and bending of O-H Of β-CD
1150.87	bending of C-O-C of β-CD	1150.31	bending of C-O-C Of β-CD
1039.00	stretching of C-C-O of β-CD	1030.00	stretching of C-C-O Of β-CD
944.27	skeletal vibration involving α-1,4linkage of β-CD	943.16	skeletal vibration involving α-1,4linkage of β-CD

Figures:

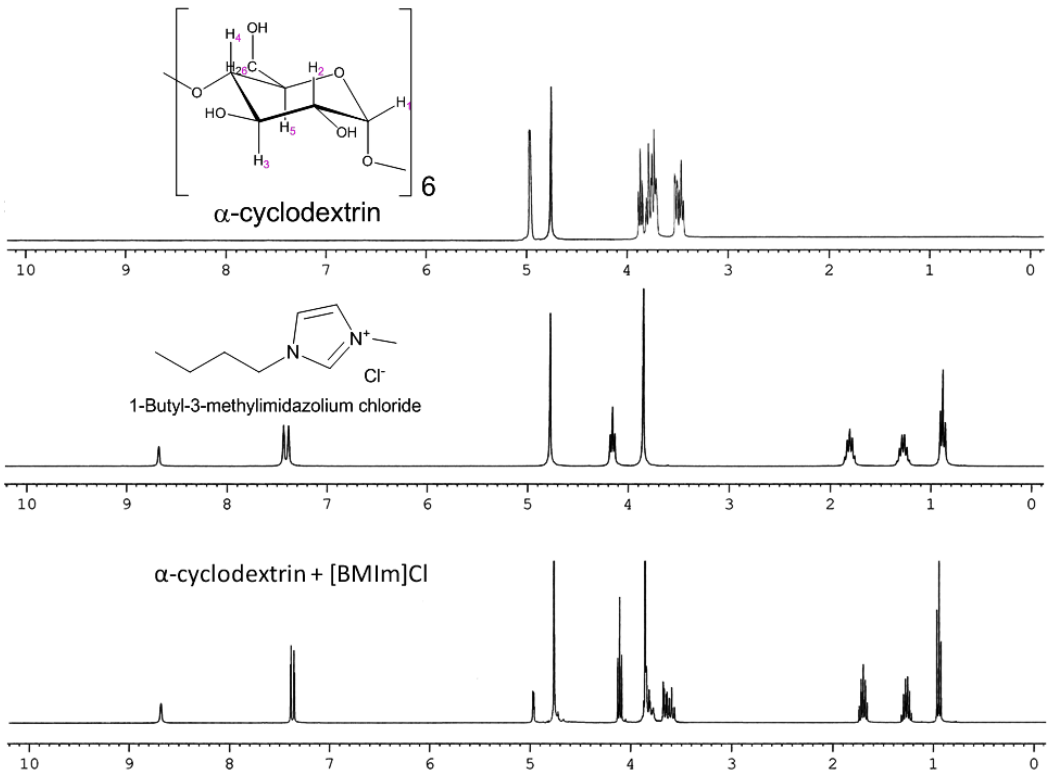

Figure IX.1. ^{1}H NMR Spectra of α-CD, [BMIm]Cl and 1:1 molar ratio of α-CD + [BMIm]Cl in D_2O in 298.15 K.

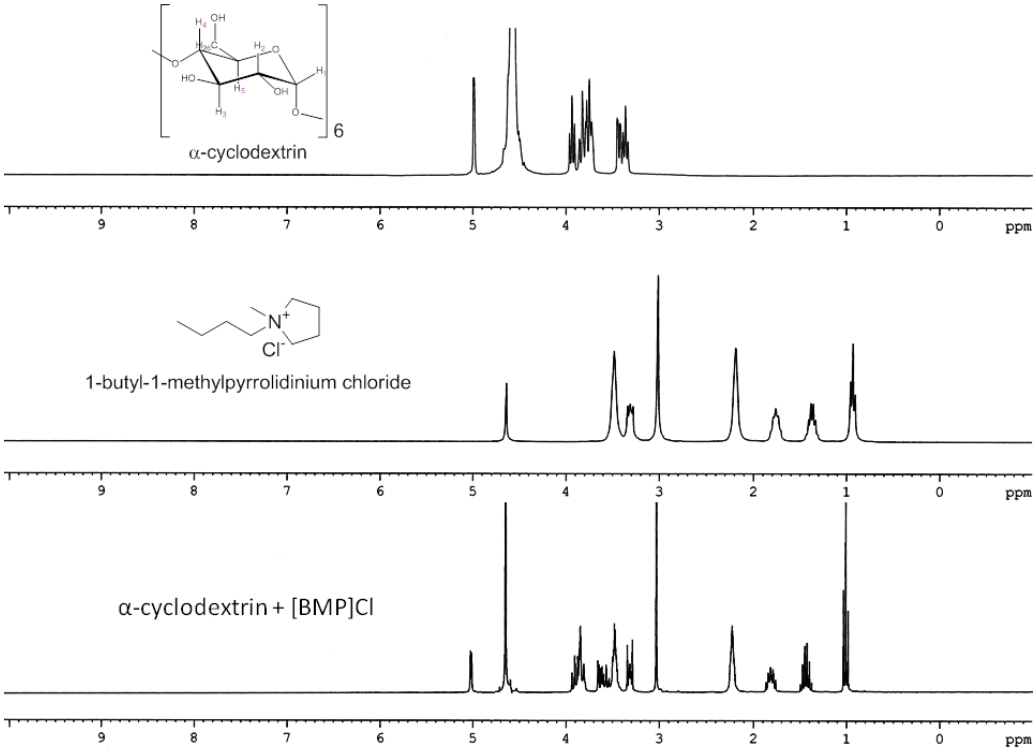

Figure IX.2. ^{1}H NMR Spectra of α-CD, [BMP]Cl and 1:1 molar ratio of α-CD + [BMP]Cl in D_2O in 298.15 K.

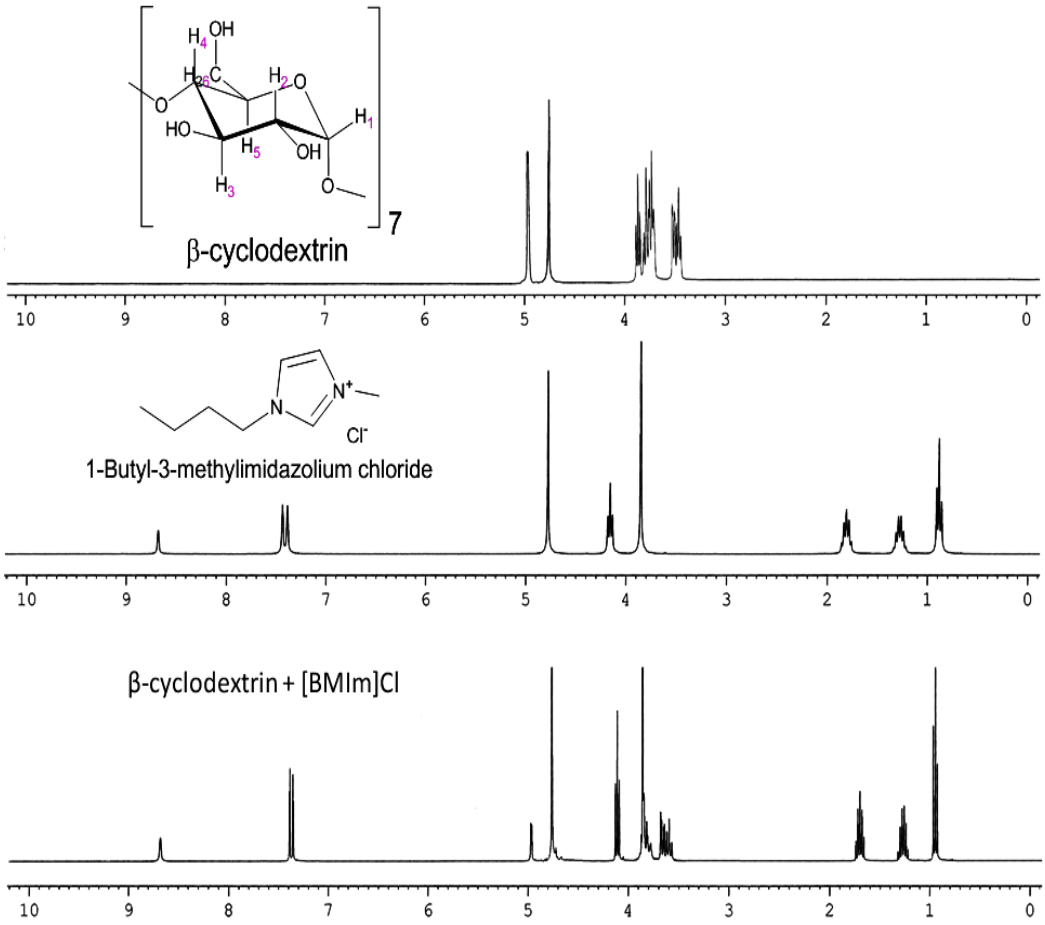

Figure IX.3. ^{1}H NMR Spectra of (a)β-CD (b) [BMIm]Cl (c) 1:1 molar ratio of β-CD and [BMIm]Cl in D_2O in 298.15 K.

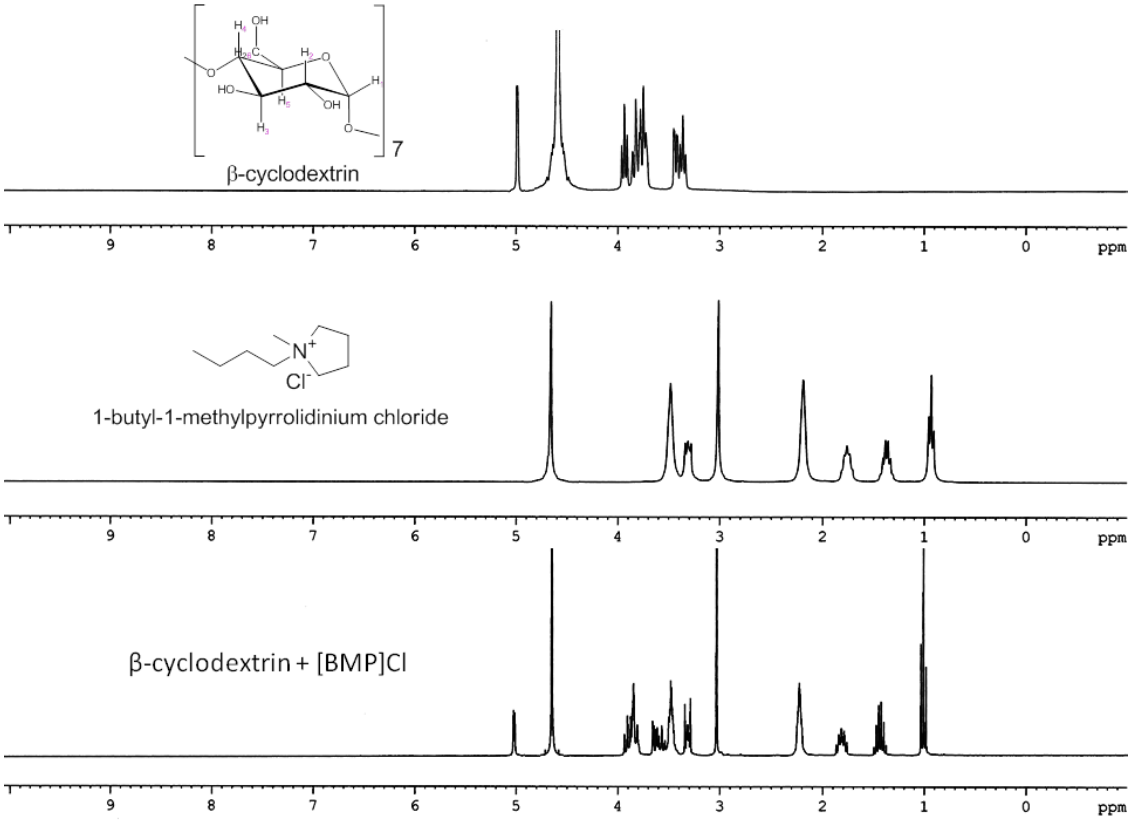

Figure IX.4. ^{1}H NMR Spectra of (a) β-CD (b) [BMP]Cl (c) 1:1 molar ratio of β-CD and [BMP]Cl in D_2O in 298.15 K.

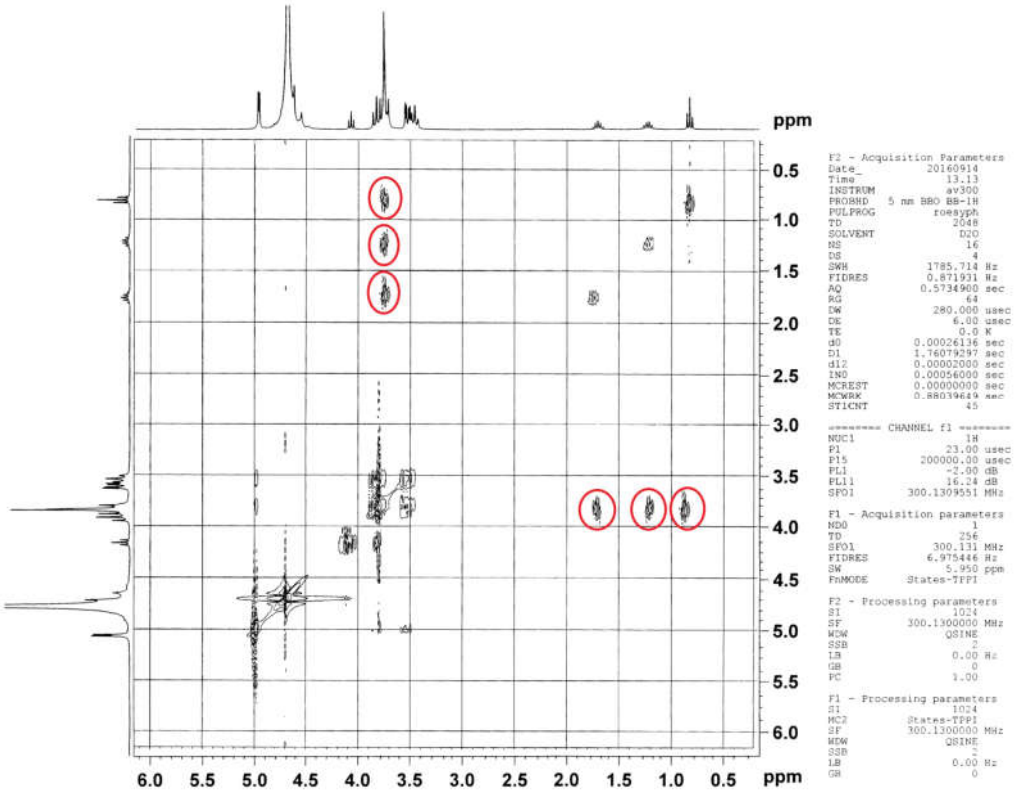

Figure IX.5. 2D ROESY spectra of solid inclusion complex of [BMIm]Cl and α-CD in D_2O (correlation signals are marked by red circles).

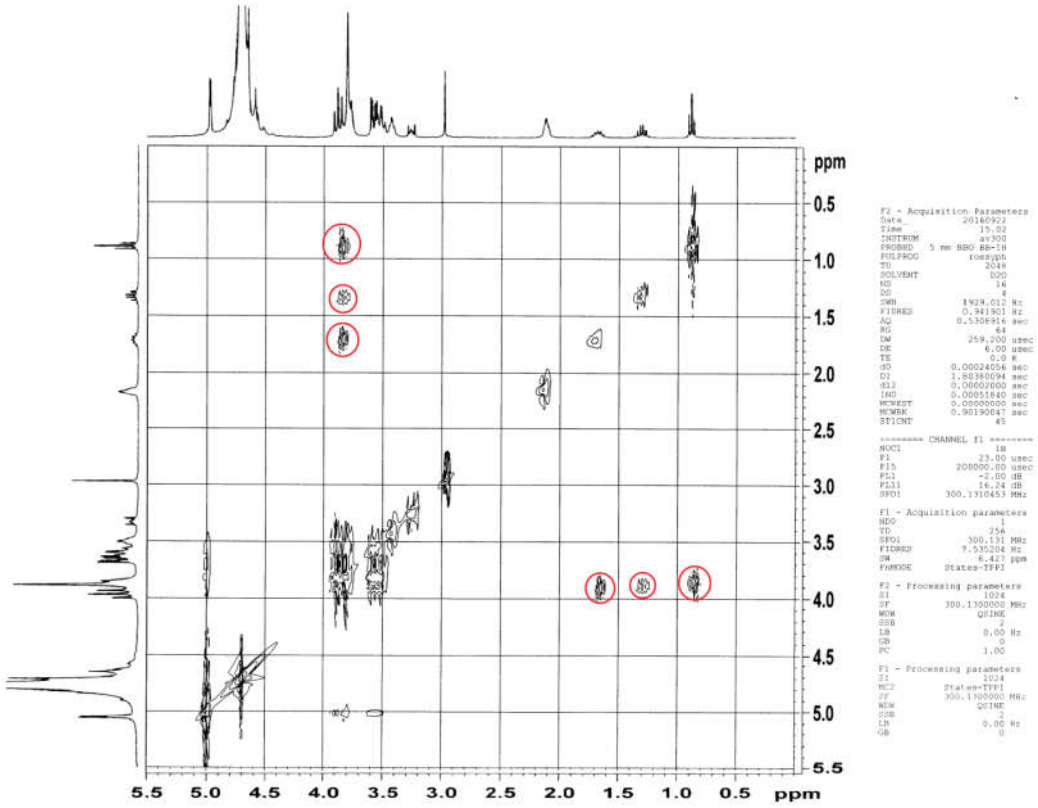

Figure IX.6. 2D ROESY spectra of solid inclusion complex of [BMP]Cl and α-CD in D_2O (correlation signals are marked by red circles).

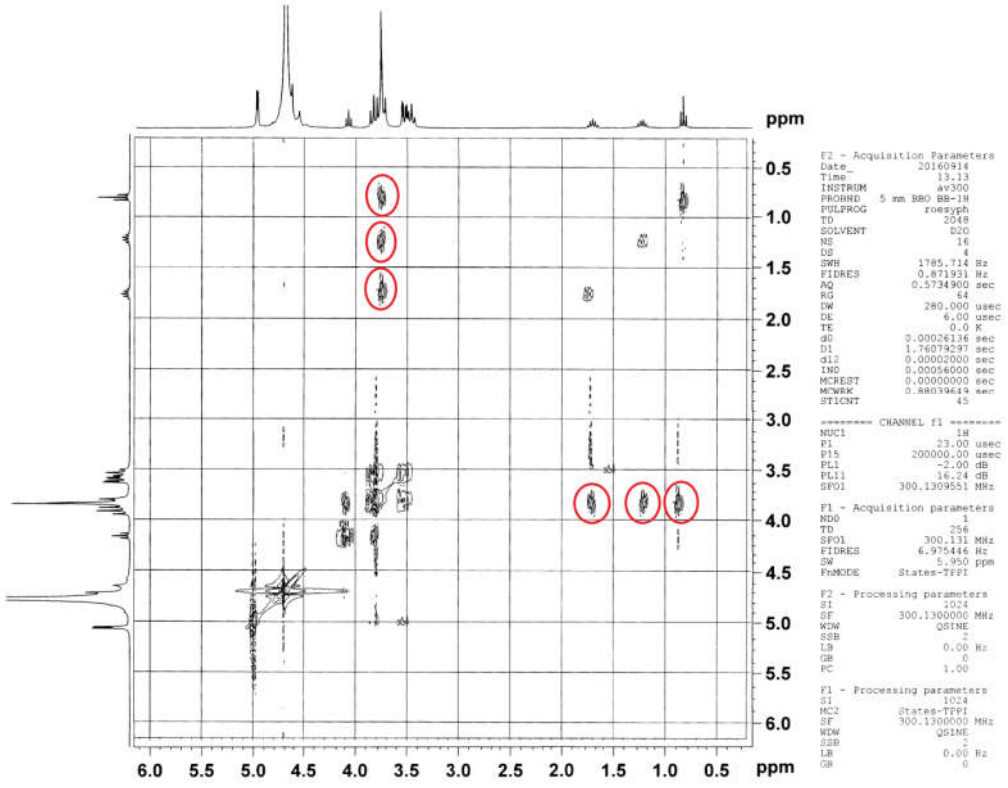

Figure IX.7. 2D ROESY spectra of solid inclusion complex of [BMIm]Cl and *β*-CD in D_2O (correlation signals are marked by red circles).

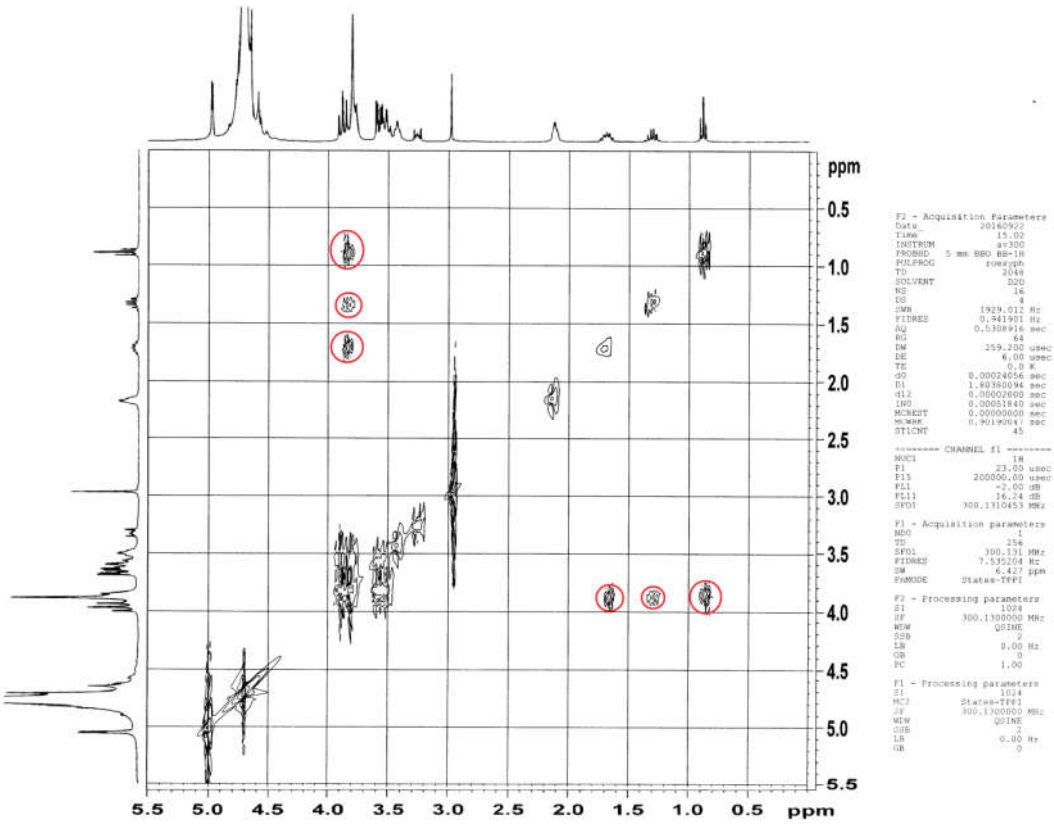

Figure IX.8. 2D ROESY spectra of solid inclusion complex of [BMP]Cl and *β*-CD in D_2O (correlation signals are marked by red circles).

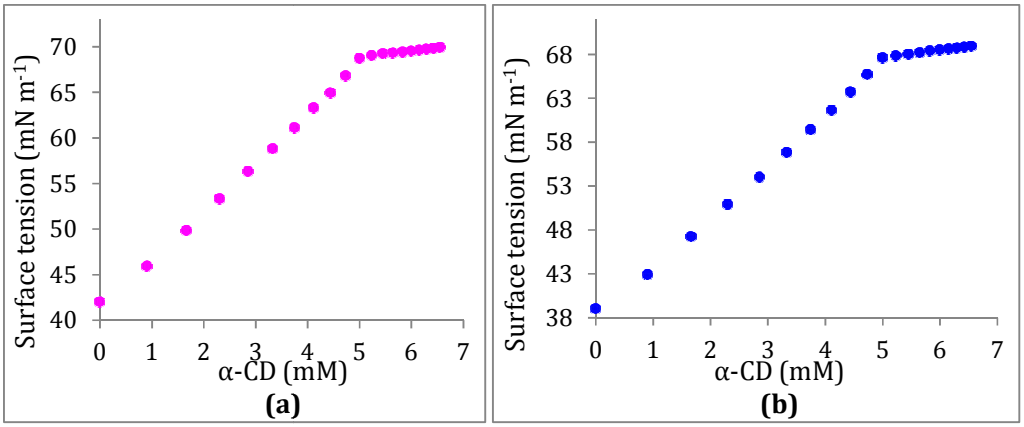

Figure IX.9. Variation of surface tension of aqueous (a) [BMIm]Cl-α-CD and (b) [BMP]Cl-α-CD systems respectively at 298.15 K.

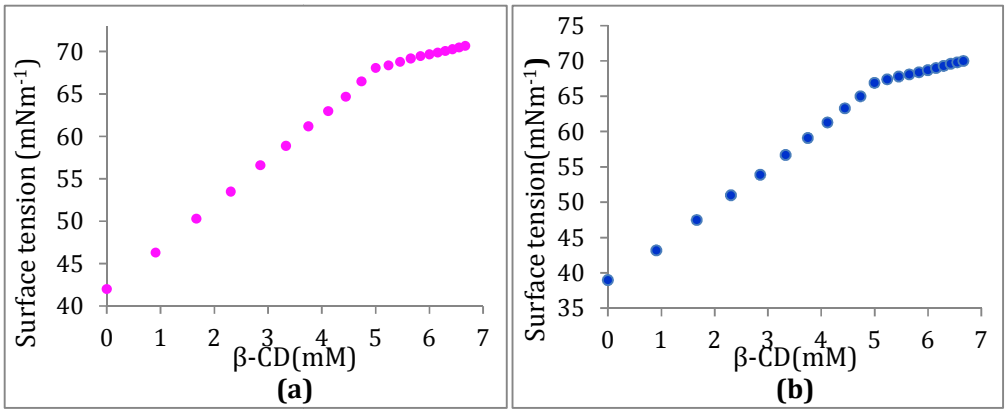

Figure IX.10. Variation of surface tension of aqueous (a) [BMIm]Cl-β-CD and (b) [BMP]Cl-β-CD systems respectively at 298.15 K.

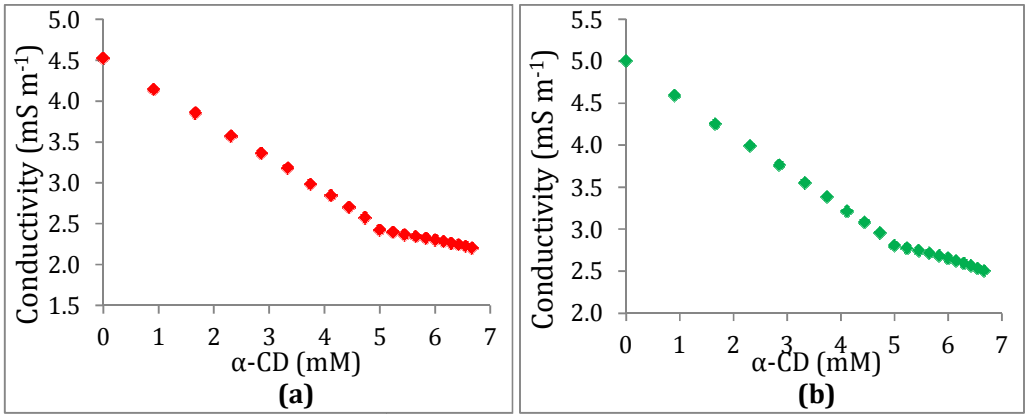

Figure IX.11. Variation of conductivity of aqueous (a) [BMIm]Cl-α-CD and (b) [BMP]Cl-α-CD systems respectively at 298.15 K.

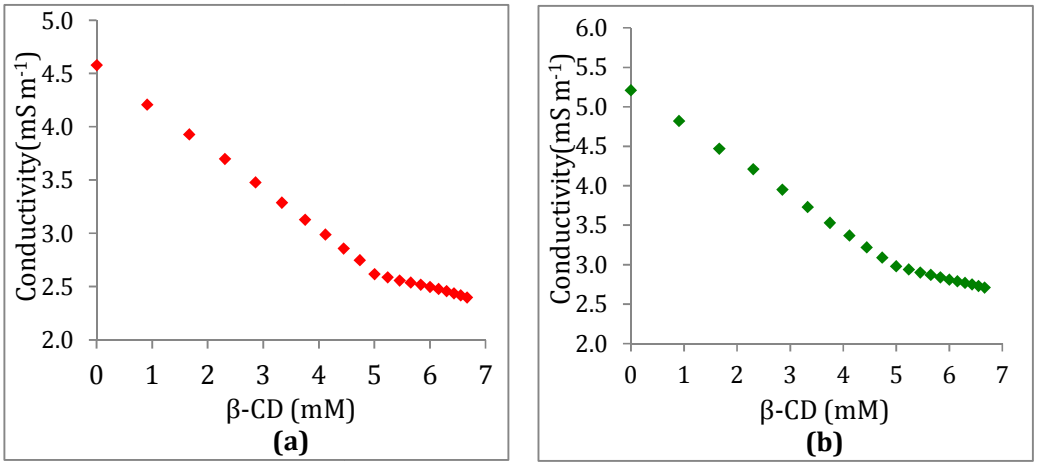

Figure IX.12. Variation of conductivity of aqueous (a) [BMIm]Cl-β-CD and (b) [BMP]Cl-β-CD systems respectively at 298.15 K.

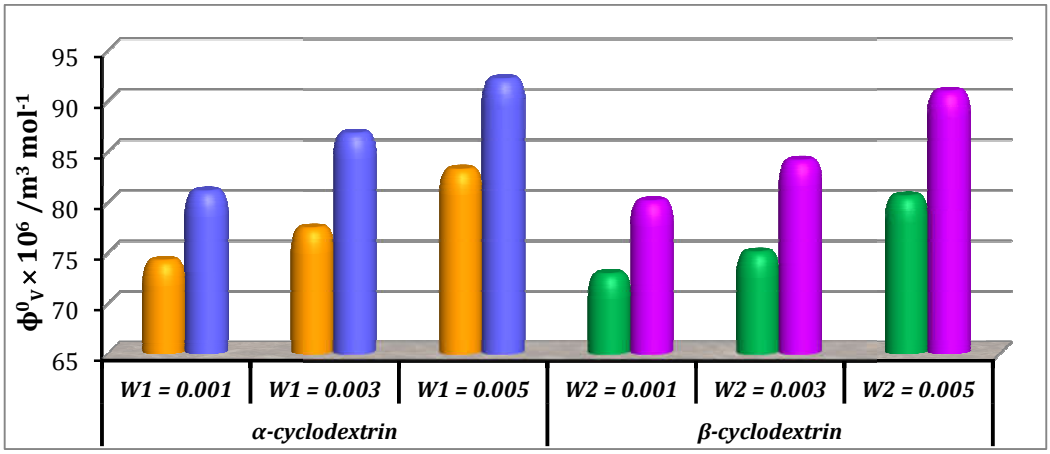

Figure IX.13. Plot of limiting molar volume (ϕ^0_V) against mass fraction (w) of aqueous α-CD and aqueous β-CD for [BMIm]Cl (orange and green) and [BMP]Cl (blue & purple) respectively at 298.15 K.

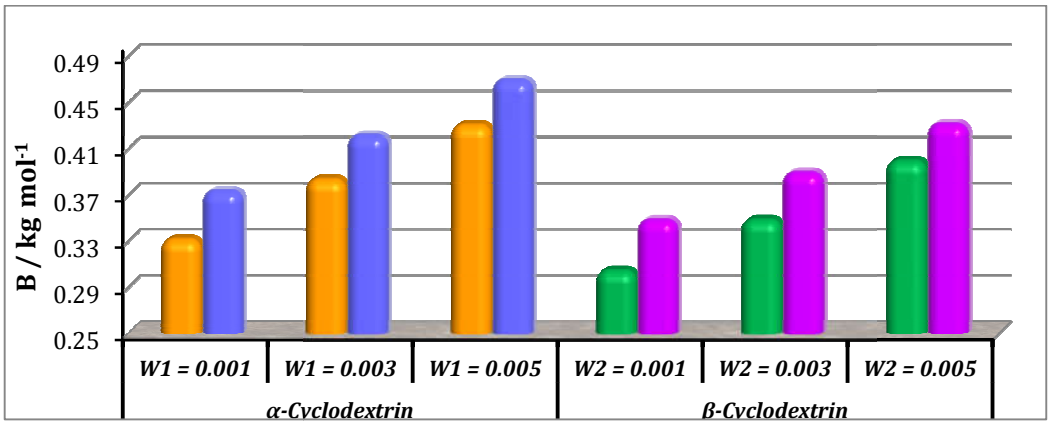

Figure IX.14. Plot of viscosity B-coefficient against mass fraction (w) of aqueous α-CD and aqeous β-CD for [BMIm]Cl (orange and green) and [BMP]Cl (blue & purple) respectively at 298.15 K.

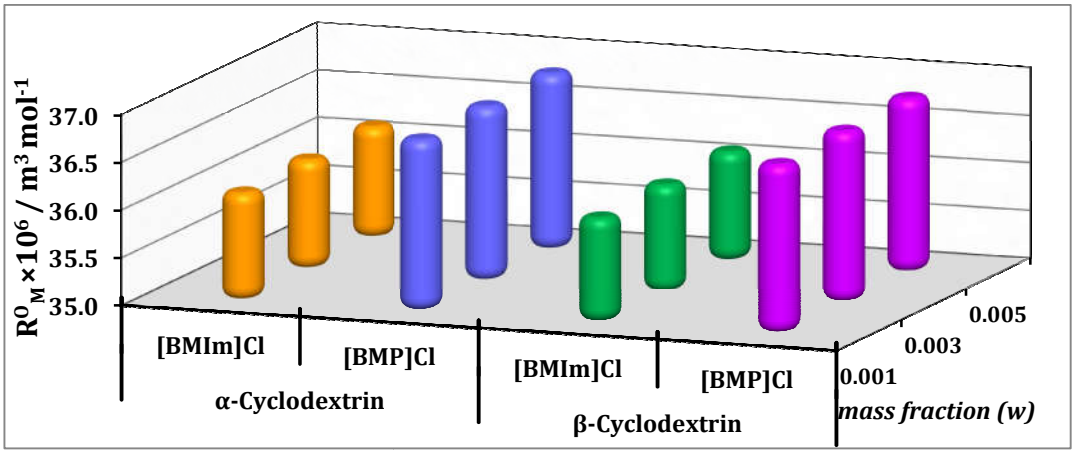

Figure IX.15. Plot of limiting molar refraction (R^0_M) for [BMIm]Cl and [BMP]Cl in different mass fractions (w) of aqueous α-CD and aqueous β-CD respectively at 298.15 K.

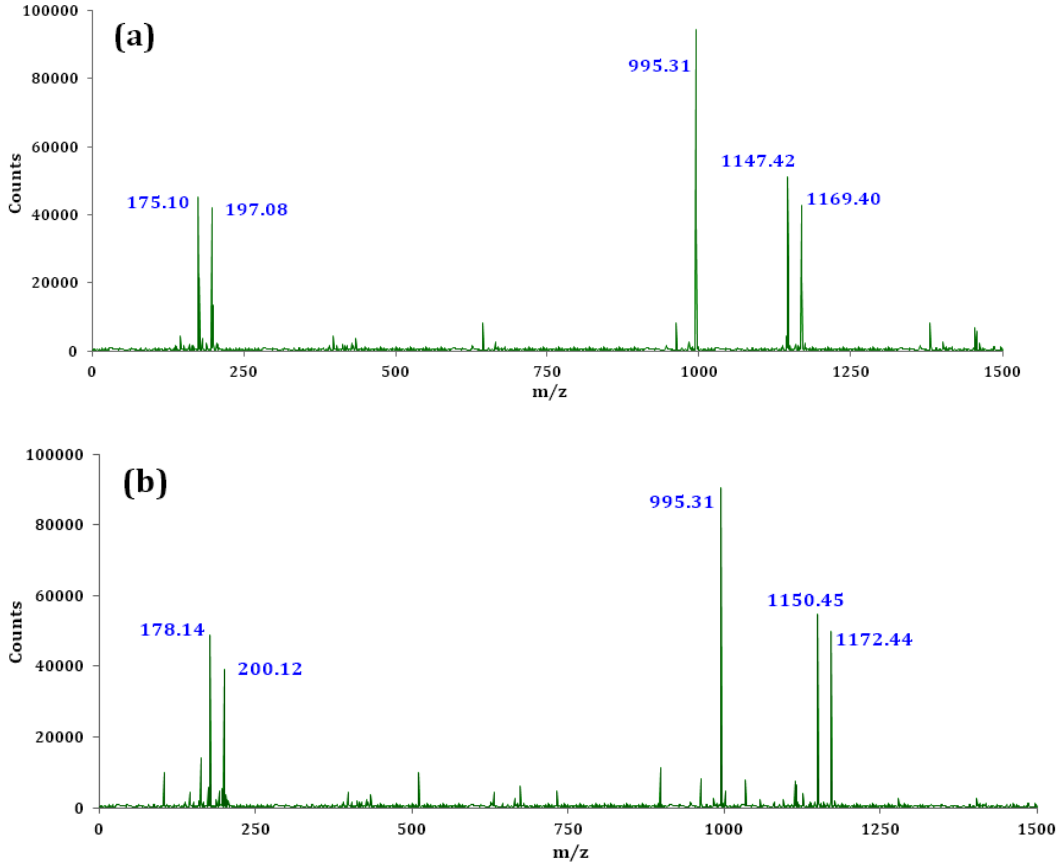

Figure IX.16. ESI mass spectra of (a) [BMIm]Cl-α-CD inclusion complex and (b) [BMP]Cl-α-CD inclusion complex.

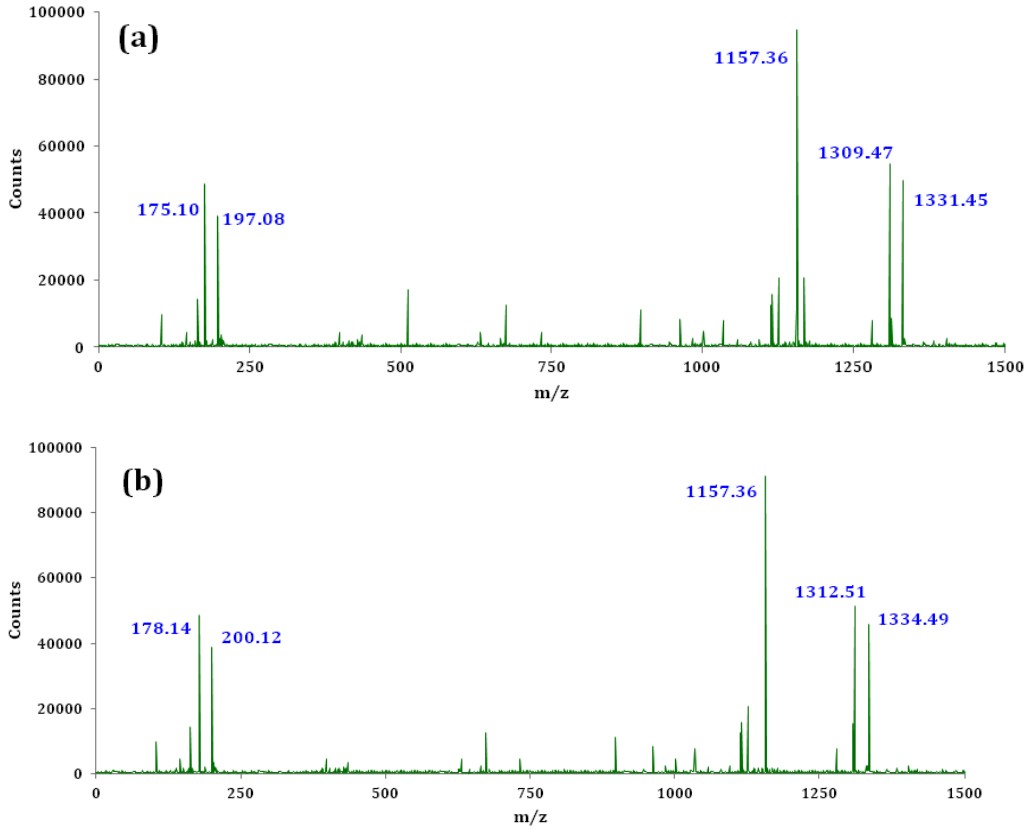

Figure IX.17. ESI mass spectra of (a) [BMIm]Cl-β-CD inclusion complex and (b) [BMP]Cl-β-CD inclusion complex.

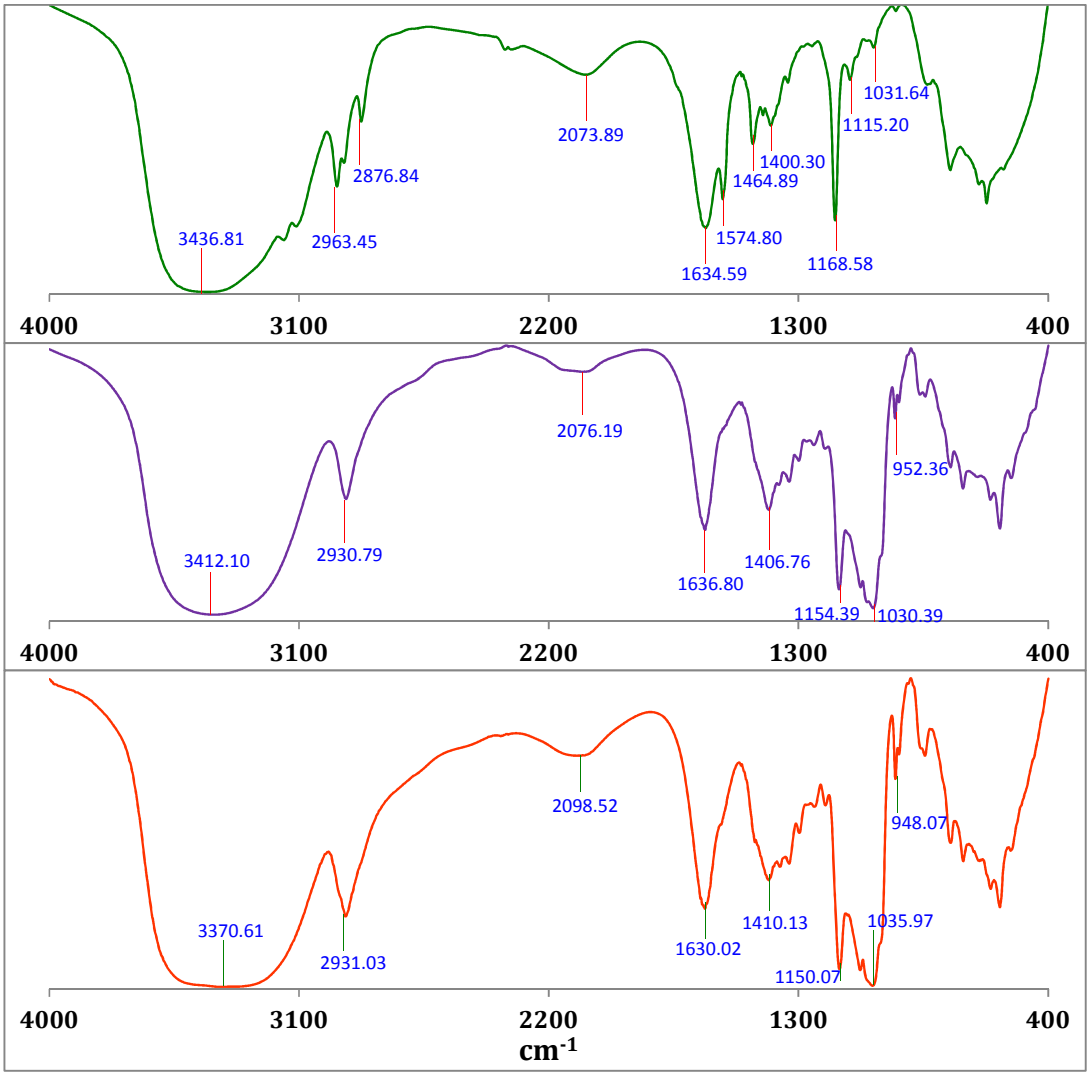

Figure VI.18. FTIR spectra of [BMIm]Cl (top), α-CD (middle) and [BMIm]Cl-α-CD inclusion complex (bottom).

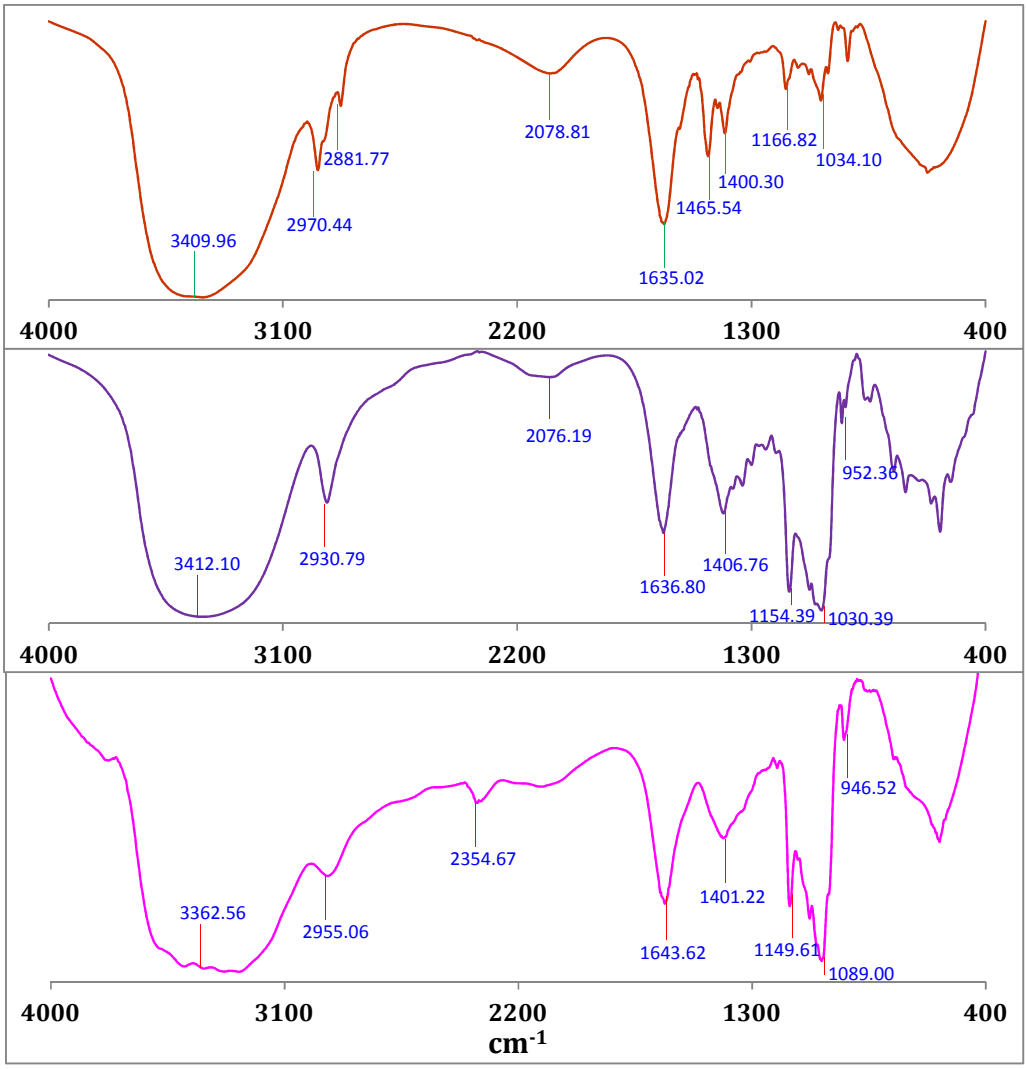

Figure VI.19. FTIR spectra of [BMP]Cl (top), α-CD (middle) and [BMP]Cl-α-CD inclusion complex (bottom).

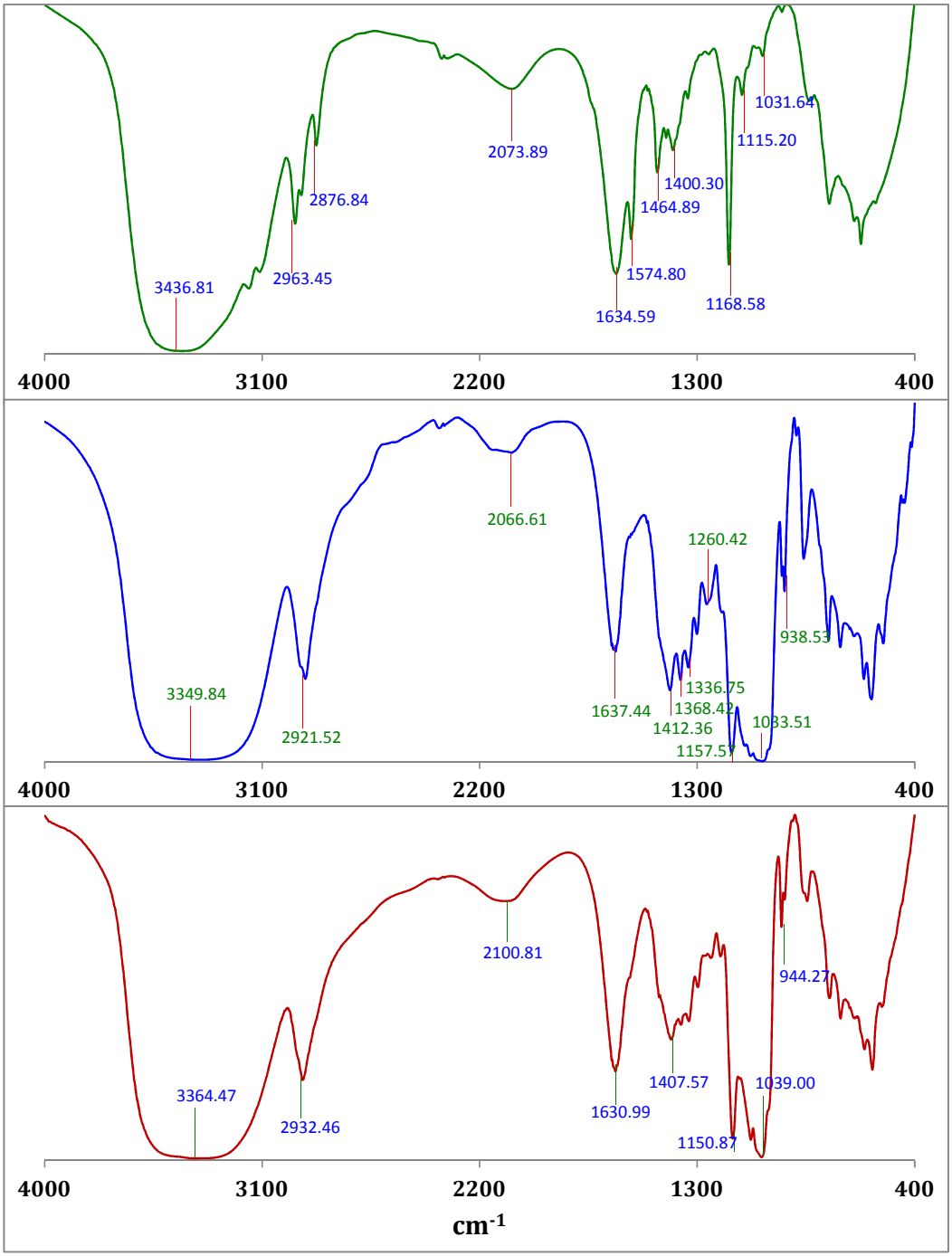

Figure VI.20. FTIR spectra of [BMIm]Cl (top), β-CD (middle) and [BMIm]Cl-β-CD inclusion complex (bottom).

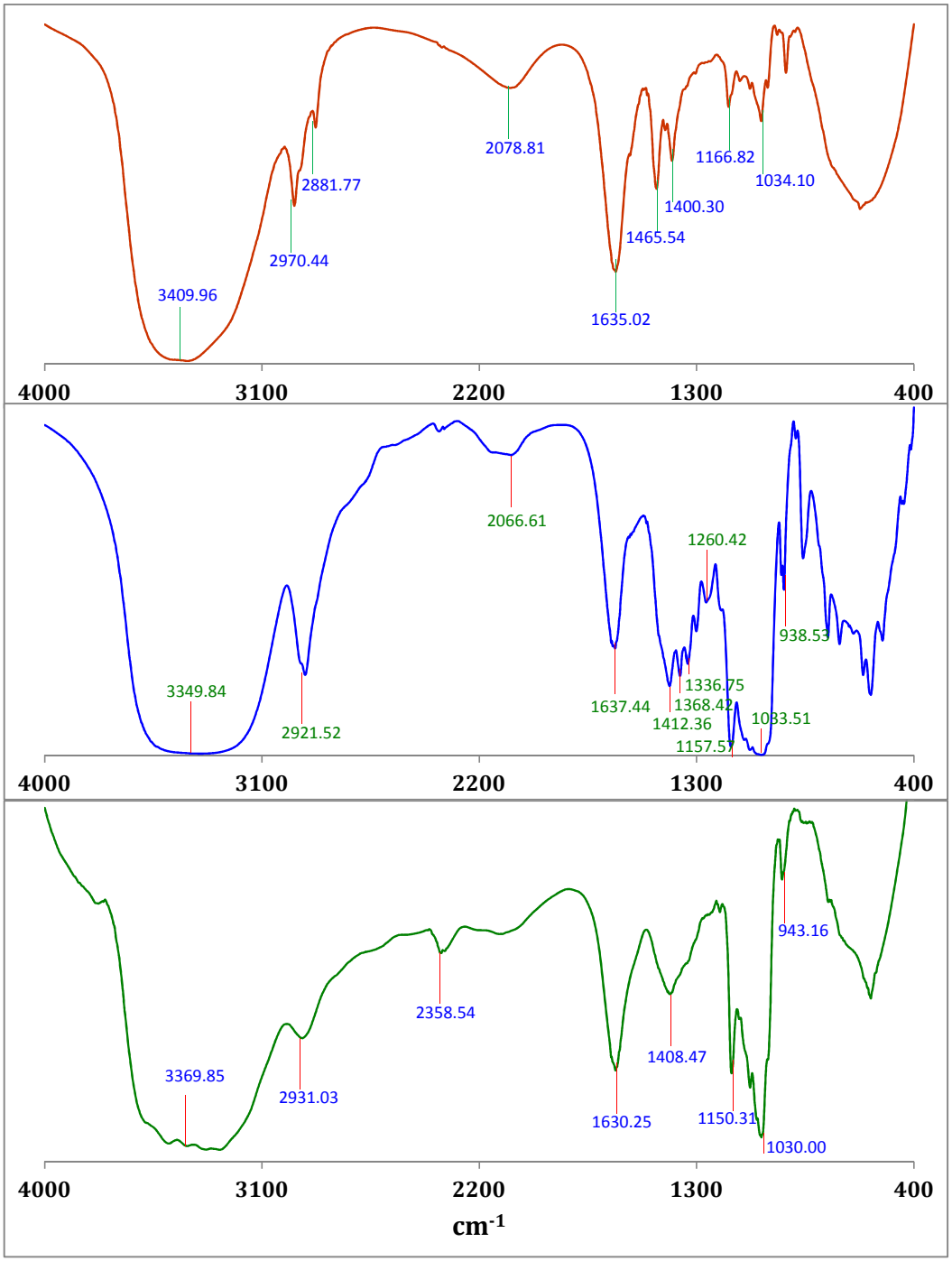

Figure VI.21. FTIR spectra of [BMP]Cl (top), β-CD (middle) and [BMP]Cl-β-CD inclusion complex (bottom).

Schemes:

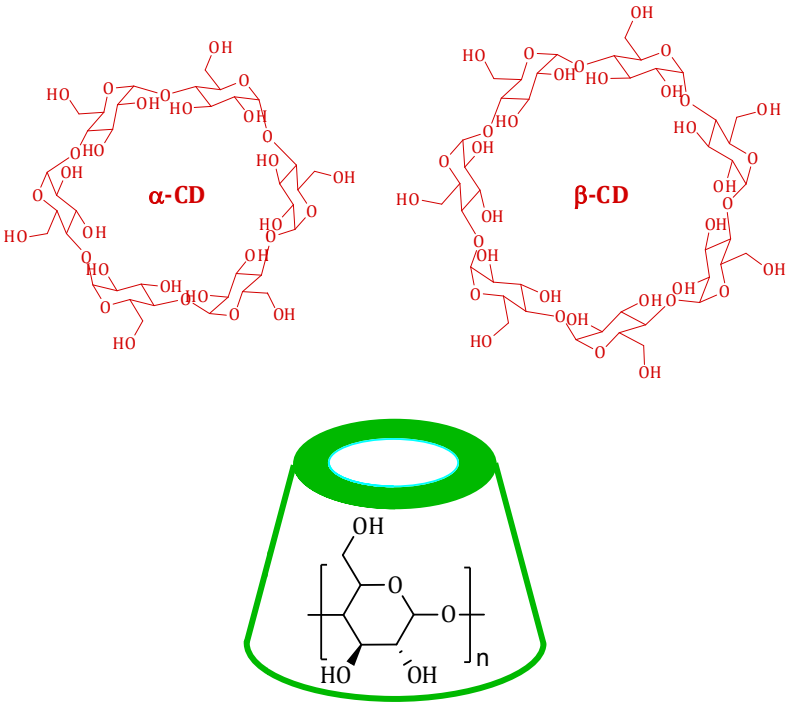

Scheme IX.1. Structure of cyclodextrin molecules.

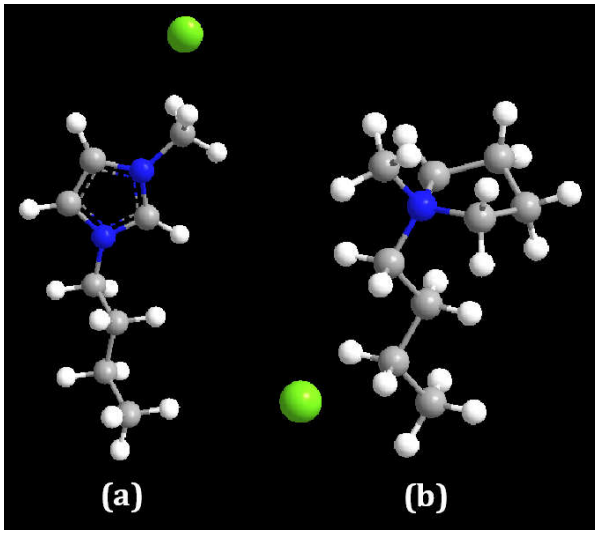

Scheme IX.2. Molecular structure of (a) [BMIm]Cl and (b) [BMP]Cl.

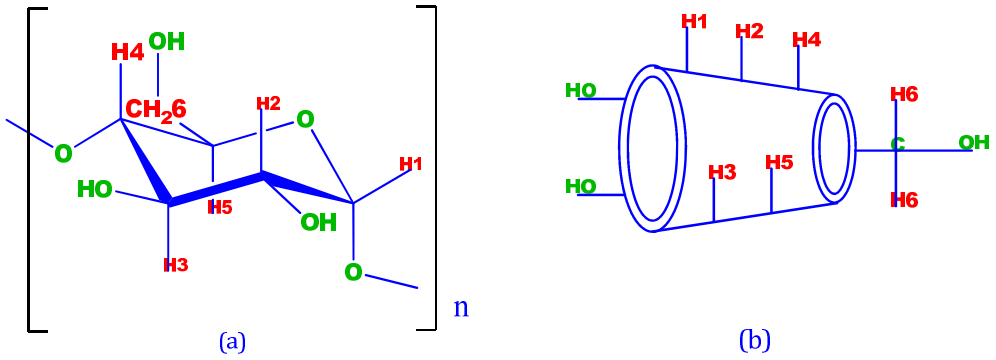

Scheme IX.3. (a) Stereochemical configuaration and (b) truncated conical structure of α and β-cyclodextrin.

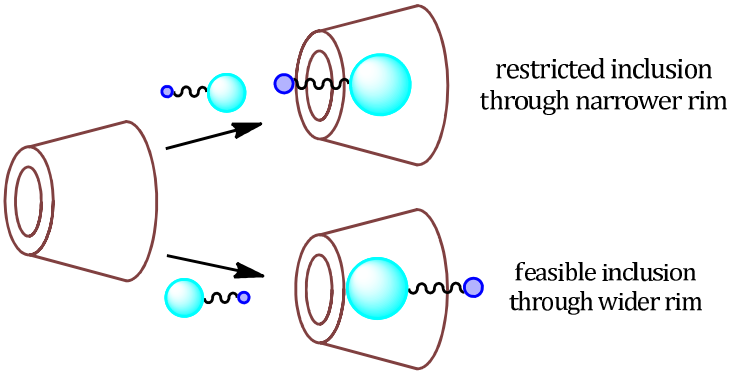

Scheme IX.4. Feasible and restricted inclusions of the guest into the host molecule.

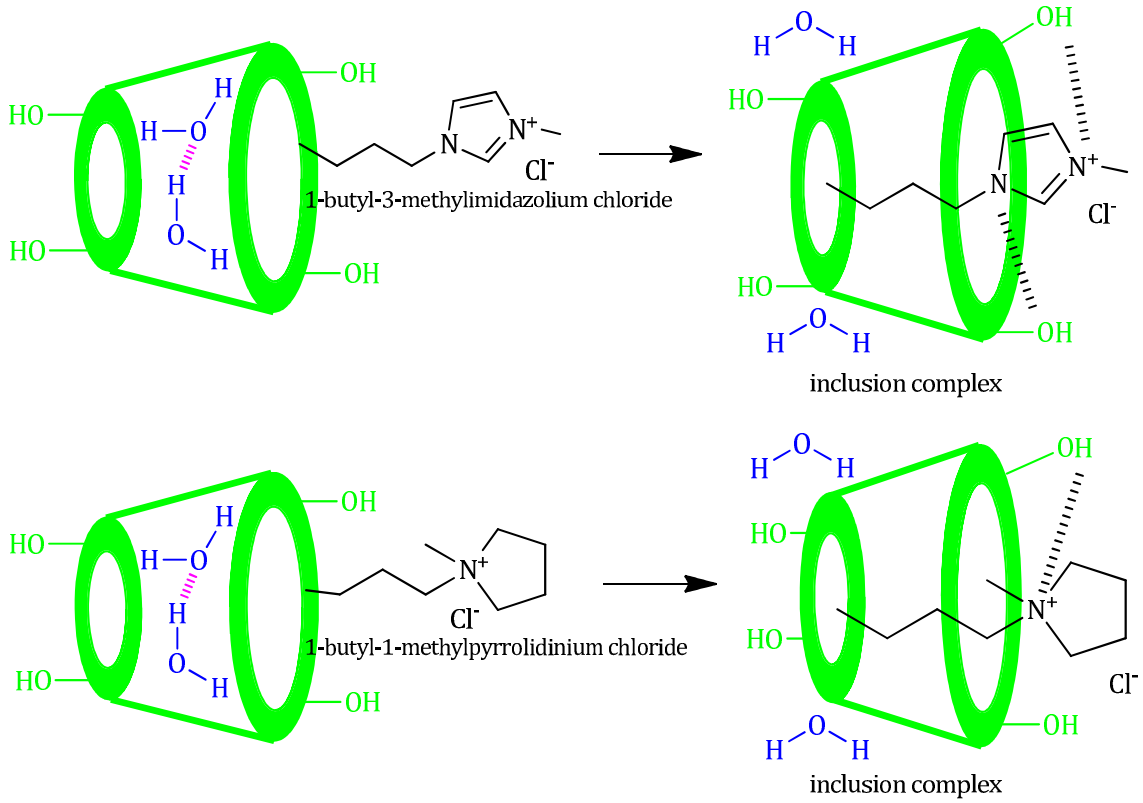

Scheme IX.5. Plausible Schematic representation of mechanism for the formation of 1 : 1 inclusion complex of [BMIm]Cl and [BMP]Cl with both α and β-cyclodextrin.

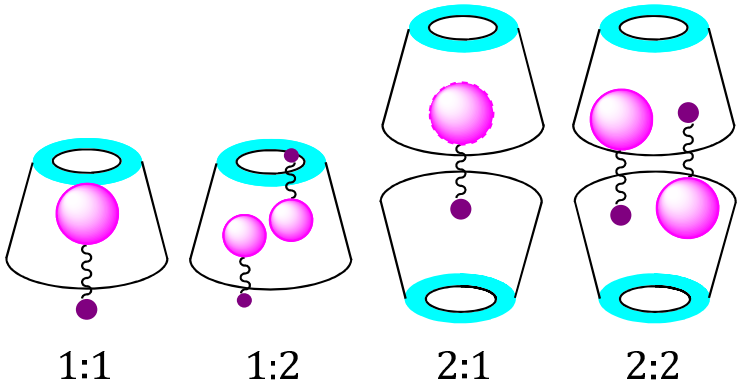

Scheme IX.6. Different stoichiometries of host-guest inclusion complexes.